Meng *et al. J. Mater. Inf.* **2025**, *5*, 3
DOI: 10.20517/jmi.2024.74

Journal of Materials Informatics

Review

Open Access

Check for updates

Superior single-atom and single-cluster catalysts towards electrocatalytic nitrogen reduction reactions: a theoretical perspective

Haihong Meng[1], Yinghe Zhao[2], Fengyu Li[2,*], Zhongfang Chen[3,*]

[1]College of Science, Inner Mongolia Agricultural University, Hohhot 010018, Inner Mongolia, China.
[2]Key Laboratory of Semiconductor Photovoltaic Technology and Energy Materials at Universities of Inner Mongolia Autonomous Region, School of Physical Science and Technology, Inner Mongolia University, Hohhot 010021, Inner Mongolia, China.
[3]Department of Chemistry, University of Puerto Rico, Rio Piedras Campus, San Juan, PR 00931, USA.

[*]**Correspondence to:** Prof. Fengyu Li, Key Laboratory of Semiconductor Photovoltaic Technology and Energy Materials at Universities of Inner Mongolia Autonomous Region, School of Physical Science and Technology, Inner Mongolia University, 235 Daxue West Street, Saihan District, Hohhot 010021, Inner Mongolia, China. E-mail: fengyuli@imu.edu.cn; Prof. Zhongfang Chen, Department of Chemistry, University of Puerto Rico, Rio Piedras Campus, 39 Avenida Ponce de Leon, San Juan, PR 00931, USA. E-mail: zhongfang.chen1@upr.edu

How to cite this article: Meng, H.; Zhao, Y.; Li, F.; Chen, Z. Superior single-atom and single-cluster catalysts towards electrocatalytic nitrogen reduction reactions: a theoretical perspective. *J. Mater. Inf.* **2025**, *5*, 3. https://dx.doi.org/10.20517/jmi.2024.74

Received: 17 Nov 2024 **First Decision:** 12 Dec 2024 **Revised:** 28 Dec 2024 **Accepted:** 4 Jan 2025 **Published:** 13 Jan 2025

Academic Editor: Lei Shen **Copy Editor:** Pei-Yun Wang **Production Editor:** Pei-Yun Wang

Abstract

The traditional Haber-Bosch process for ammonia synthesis is both energy-intensive and capital-demanding. Electrocatalytic nitrogen reduction reaction (NRR) has emerged as a promising, sustainable alternative, with recent advantages highlighting its potential. Single-atom catalysts (SACs) and single-cluster catalysts (SCCs) are promising catalysts for NRR due to their atomically dispersed active sites, maximized atom utilization, and distinctive coordination and electronic structures, all of which facilitate mechanism insights at the atomic level. Benefiting from efficient atom utilization, for example, the ammonia yield rate on Au_1/C_3N_4 is roughly 22.5 times as high as that of supported Au nanoparticles, fully demonstrating the significant advantages of SACs over nanoparticles. In this review, we focus on the theoretical progress in SACs and SCCs for electrocatalyzing NRR, including nitrogenase-like bio-inspired catalysts and other metal-based catalysts. We further examine key adsorption energy and electronic descriptors that enhance our understanding of catalytic performance. Finally, we discuss the remaining challenges and future directions for advancing SACs and SCCs in electrocatalytic NRR applications.

Keywords: Nitrogen reduction reaction, electrocatalysts, single-atom catalysts, single-cluster catalysts, theoretical perspective

INTRODUCTION

Though atomic dispersion of transition metal (TM) had been recognized for its excellent catalytic activity[1-3], the term "single-atom catalysts (SACs)" was formally coined by Zhang *et al.* in 2011[4]. SACs exhibit superior catalytic performance across a wide range of reactions compared with traditional catalysts, mainly due to their unsaturated coordination and unique electronic structures, which enhance both catalytic activity and atom economy[5]. The presence of single active sites in SACs also facilitates the investigation of structure-activity relationships at the molecular and atomic levels, bridging the gap between homogeneous and heterogeneous catalysis. Consequently, within just a few years of their introduction, SACs have rapidly emerged as a research frontier in catalysis and successfully applied to various energy-related reactions[6-10].

The seminal article by Zhang *et al.* has now been cited over 5,500 times, underscoring the impact and growing attention that SACs have received within the catalysis community, as illustrated in Figure 1.

Exciting progress has been made in high-performance electrocatalytic SACs. However, breaking the linear scaling relationship between the adsorption energy of reaction intermediates remains challenging due to the single-atom active sites, which fundamentally limits further improvement in catalytic efficiency. Compared to SACs, single-cluster catalysts (SCCs) offer multiple active centers and more flexible adsorption configurations, allowing intermediates to adsorb at different active centers. This flexibility is expected to overcome the limitations imposed by the linear scaling relationship[11,12].

Moreover, the synergistic interaction between multiple metal atoms in SCCs can modulate the electronic structure, providing enhanced catalytic activity from different perspectives. Last but not least, the well-defined structure of SCCs facilitates the study of structure-performance relationships and catalytic mechanisms. In recent years, researchers have explored SCCs derived from SACs, mainly focusing on simple diatomic and triatomic catalysts (DACs and TACs)[13-15].

Nitrogen, the most abundant gas in Earth's atmosphere (more than 78%), plays a crucial role in various industrial processes[16]. The industrial production of ammonia (NH_3) via the Haber Bosch process, however, is energy-intensive and contributes significantly to environmental pollution[17]. Thus, the exploration of sustainable and green ammonia synthesis methods has been a research hotspot in recent years.

Significant efforts have been dedicated to developing high-performance electrocatalysts for the nitrogen reduction reaction (NRR)[18]. With regard to NRR, recently emerged SACs and SCCs have shown promise, demonstrating remarkable performance under mild conditions[19-21]. Theoretical calculations, which serve as a guiding tool for designing novel and efficient electrocatalysts, are both time- and cost-effective, greatly facilitating the screening of numerous potential catalysts without experimental effort.

This review summarizes recent theoretical and computational efforts in SACs and SCCs toward electrocatalytic ammonia synthesis. First, we introduce the typical reaction mechanisms. Next, we elaborate on the latest research progress of SACs towards NRR, classified by the elements of the active components, and present recent research on SCCs for NRR. Then, we discuss activity descriptors in detail. Finally, we highlight some existing challenges and outline future directions to achieve further breakthroughs in NRR and other multi-electron reactions, focusing on enhancing catalytic performance and selectivity.

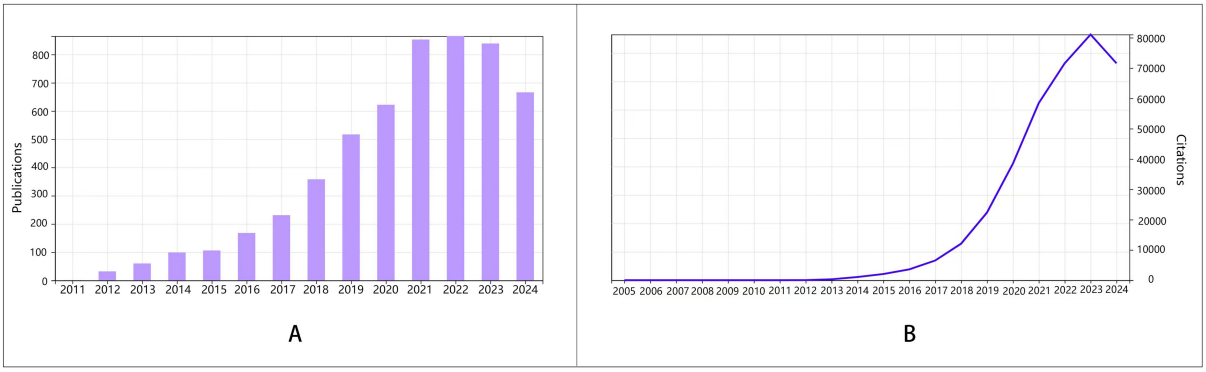

Figure 1. (A) Publications and (B) citations based on the seminal article by Zhang *et al.* on SACs, retrieved from the Web of Science website on October 30, 2024. SACs: Single-atom catalysts.

BRIEF INTRODUCTION TO THE NRR REACTION MECHANISM

The reaction mechanisms for NRR vary depending on the type and structure of the catalysts. Conventional mechanisms include dissociative (DM) and associative mechanisms (AM). In the DM, the N≡N triple bond is completely broken at the active site before hydrogenation occurs, similar to the traditional Haber-Bosch process. AMs can be further categorized into consecutive, distal, alternating, enzymatic, and continuous pathways, depending on the mode of N_2 adsorption and hydrogenation [Figure 2A].

For the N_2 end-on adsorption configuration, the distal mechanism involves hydrogenating the nitrogen atom furthest from the active center to form NH_3, while the alternating mechanism involves hydrogenating both nitrogen atoms in succession. In the enzymatic and consecutive mechanisms, the hydrogenation of side-on adsorbed N_2 is similar to the alternating and distal mechanisms, respectively, except that N_2 is adsorbed in a side-on configuration. Additionally, the Mars-van-Krevelen (MvK) mechanism, proposed by Skúlason and Abghoui[28-30], involves the reduction of a surface N atom to NH_3, followed by a reformation of the nitrogen-vacancy, particularly in TM nitrides (TMNs) [Figure 2B].

Qu *et al.* discovered a novel enzyme-distal mechanism in which the potential-determining step is the transition from $^*NH_2$ to NH_3 [Figure 2C]. This process occurs because both the lone pairs of electrons and the unbonded sp^3 electrons in N atoms in SAC@MXene systems can be coordinated with single metal atomic sites. During the final hydrogenation step, the SAC-N interaction is disrupted, and a new N–H σ bond is formed, resulting in an uphill change in energy. By weakening the SAC–N bond, the adsorption of $^*N$, $^*NH_2$, and $^*NH_3$ species is also weakened, thereby achieving a lower limiting potential (U_L)[24].

More recently, Wang *et al.* designed a localized dual-active site catalyst that successfully broke the linear relationship of traditional systems[25]. They proposed a new mechanism involving the co-activation of N_2 at both ends. Following this mechanism, two weakly adsorbed N atoms are effectively activated and the N≡N triple bond is cleaved, with each N atom binding to separate weakly adsorbed metal centers, thus facilitating subsequent hydrogenation steps [Figure 2D].

Notably, Wang *et al.* introduced another novel mechanism, where two $^*N_2H_2$ species desorbed from a Rh surface and subsequently decomposed into NH_3 and N_2 [Figure 2E][26]. In addition to the DMs or AMs described above, they proposed a surface-hydrogenation mechanism where N_2 is activated and reduced to $^*N_2H_2$ by surface $^*H$, with hydrogen reduction occurring as the initial step rather than N_2 adsorption [Figure 2F][27].

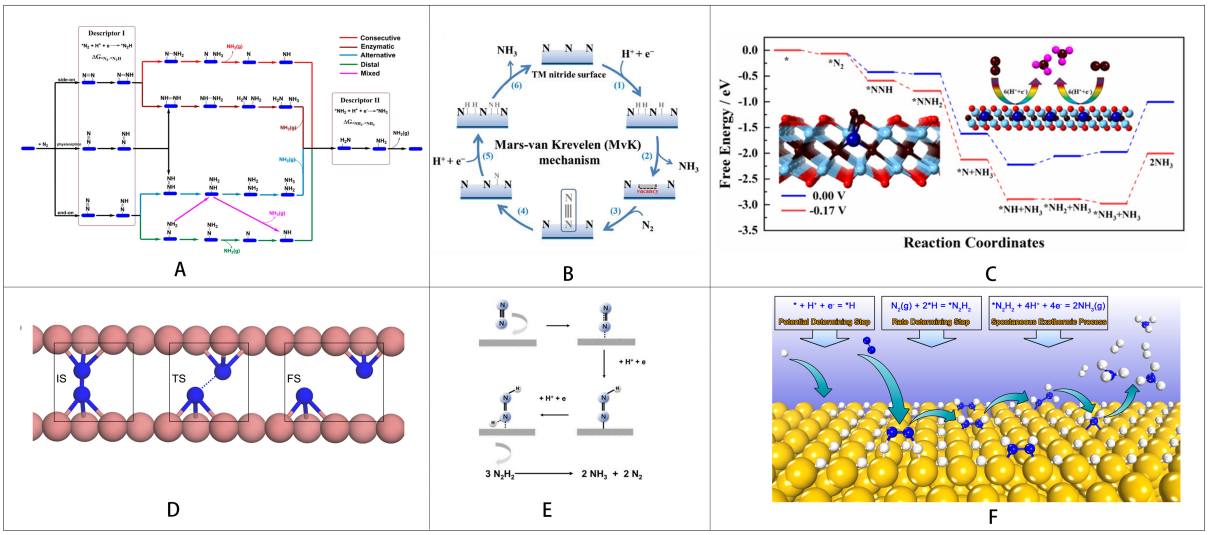

Figure 2. (A) Schematic illustration of five possible mechanisms (consecutive, enzymatic, alternative, distal, and mixed) for NRR. Reprinted with permission from Ref.[22]. Copyright © 2021, American Chemical Society; (B) MvK mechanism for NRR. Reprinted with permission from Ref.[23]. Copyright © 2019 WILEY-VCH Verlag GmbH & Co. KGaA, Weinheim; (C) Enzyme-distal mechanism for NRR. Reprinted with permission from Ref.[24]. Copyright © 2021 Dalian Institute of Chemical Physics, the Chinese Academy of Sciences; (D) N_2 dissociation mechanism under confined dual sites (pink and blue spheres denote metal and nitrogen atoms, respectively; IS, TS, and FS denote initial, transition, and final states, respectively). Reprinted with permission from Ref.[25]. Copyright © 2024 National Academy of Sciences; (E) Reaction mechanism for NRR on Rh surface. Reprinted with permission from Ref.[26]. Copyright © 2020 Wiley-VCH Verlag GmbH & Co. KGaA, Weinheim; (F) Schematic of surface-hydrogenation mechanism for NRR on noble-metal-based catalysts. Reprinted with permission from Ref.[27]. Copyright © 2019 American Chemical Society. NRR: Nitrogen reduction reaction; MvK: Mars-van-Krevelen; IS: initial state; TS: transition state; FS: final state.

SACS TOWARDS NRR

Mo-based SACs

In nature, nitrogenase enzymes convert N_2 to NH_3 under mild conditions (< 40 °C, atmospheric pressure)[31]. Unfortunately, biological nitrogenases are significantly influenced by environmental factors, leading to instability in nitrogen fixation and limiting their large-scale applications. The active center of nitrogenase systems comprises clusters of different metal atoms, such as Fe-Mo, V-Fe, and Fe-Fe nitrogenases. Naturally, bio-inspired catalyst structures containing Mo, Fe, or V atoms deposited on two-dimensional (2D) nanomaterials have been extensively explored for their catalytic performance under mild conditions.

Recent reports on Mo/Fe/V-based SACs towards NRR, calculated using first-principles methods, are summarized in Table 1. Among these systems, the Fe-Mo nitrogenase systems have received the most attention, leading to the design of various Mo-containing catalysts for NRR. Thus, in this subsection, we focus on Mo-based SACs, highlighting representative catalysts.

Zhao *et al.* systematically investigated the potential of a series of single TM atoms (Sc ~ Zn, Nb, Mo, Rh, Ru, Pd, and Ag) anchored on the BN monolayers with a boron monovacancy (TM-BN) and on C_2N monolayer (TM@C_2N) as NRR catalysts by density functional theory (DFT) calculations. The results showed that Mo-BN [Figure 3A] and Mo@C_2N are promising NRR catalysts with low U_L of -0.35 and -0.17 V, respectively[32,33]. In addition, Zhao *et al.* systematically studied the activity of single atoms of Sc, Ti, V, Cr, Mn, Fe, Co, Ni, Cu, Mo, Rh, and Ru embedded on MoS_2 nanosheets with S-vacancy defects (TM/MoS_2) as NRR catalysts. It is indicated that Mo/MoS_2 nanosheet exhibits the highest NRR activity due to the high stability of $^*N_2H$ intermediates[34]. These findings suggest that the choice of substrate material significantly

Table 1. Summary of the Mo/Fe/V-based SACs towards NRR investigated by DFT calculations

Systems	Limiting potential/V	Reaction mechanism	Year of publication
Mo-BN	-0.35	Enzymatic	2017[32]
Mo@C_2N	-0.17	Distal	2018[33]
Mo-MoS_2	-0.53	Distal/alternating	2018[34]
Mo@GDY	-0.33	Distal	2020[35]
Mo-Pp	-0.58	Distal/alternating	2020[36]
Mo@BM-β_{12}	-0.26	Enzymatic	2021[37]
Mo@BM-α	-0.32	Enzymatic	2022[38]
Mo_1-N_1C_2	-0.40	Enzymatic	2018[39]
Mo_1/N_3-G	-0.50	Distal-to-alternating hybrid	2019[40]
MoN_3@555-777 graphene	-0.57 -0.57	Distal Enzymatic	2020[41]
Mo/*g*-CN	-0.39	Distal	2020[42]
Mo-MoSSe with S vacancy	-0.49	Alternating	2019[43]
Mo-based MOFs	-0.34	Distal/alternating	2019[44]
Mo@BCN	-0.59	Enzymatic	2019[45]
Mo/G with Se doping	-0.41	Enzymatic	2019[46]
Mo_1N_3-BP	-0.18	Distal	2019[47]
Mo/CeO_2-S	-0.52	Distal/alternating	2019[48]
Mo-PTA	-0.42	Distal	2019[49]
Mo_1-PMA	-0.35	Enzymatic	2022[50]
FeB_6 (β)	-0.68	Distal	2019[51]
V@BN	-0.41	Enzymatic	2020[52]
V_1@Ti_2CO_2	-0.20	Mixed	2023[53]
V@*g*-C_3N_4	-0.55	Distal	2023[54]
Fe-C_2N	-0.7	Distal/alternating	2020[55]
Ti@N_4 V@N_4	-0.69 -0.87	Distal Distal	2018[56]
V/β_{12}-BM	-0.28	Enzymatic	2019[57]
V@GDY	-0.67	Distal/alternating	2020[58]
V/Ars	-0.26	Enzymatic	2020[59]

SACs: Single-atom catalysts; NRR: nitrogen reduction reaction; DFT: density functional theory; GDY: graphdiyne monolayer; Pp: porphyrin; BM-β_{12}: metal-doped β-borophene; BM-α: metal-doped α-borophene; N_1C_2: N-doped carbon; N_3-G: N-doped graphene; MOFs: metal-organic frameworks; N_3-BP: N-doped black phosphorus; PTA: phosphotungstic acid; PMA: phosphomolybdic acid; Ti@N_4: Ti on defective graphene derivatives; V-β_{12}-BM: V anchored on boron monolayer (β_{12}); Ars: arsenene nanosheet.

influences catalytic activity due to differences in the coordination environment of the Mo center. Specifically, the intrinsic nitrogen reduction catalytic activity and selectivity of SACs are strongly influenced by the surrounding environment of the active metal atoms and the geometry of the support, just as they are in the oxygen reduction reaction (ORR)[60].

Mo-based SACs supported by graphene-like 2D materials are expected to combine the advantages of Mo atoms (the active center of natural nitrogenase) and 2D substrates (acting as electron bridges and reservoirs), showing great potential for NRR applications. Zhai *et al.* reported that Mo embedded in a graphdiyne (GDY) monolayer (Mo@GDY) [Figure 3B] stood out among a series of TM-embedded GDY monolayer (TM@GDY, TM = Sc, Cr, Mn, Fe, Co, Ni, Cu, Zn, Mo, Ru, Rh, Pd, and Ag), exhibiting high stability, excellent conductivity, and superior NRR activity through the distal mechanism. This behavior was attributed to the strong interactions between hydrogen and the neighboring nitrogen atoms (H-N_2) during the first hydrogenation step[35].

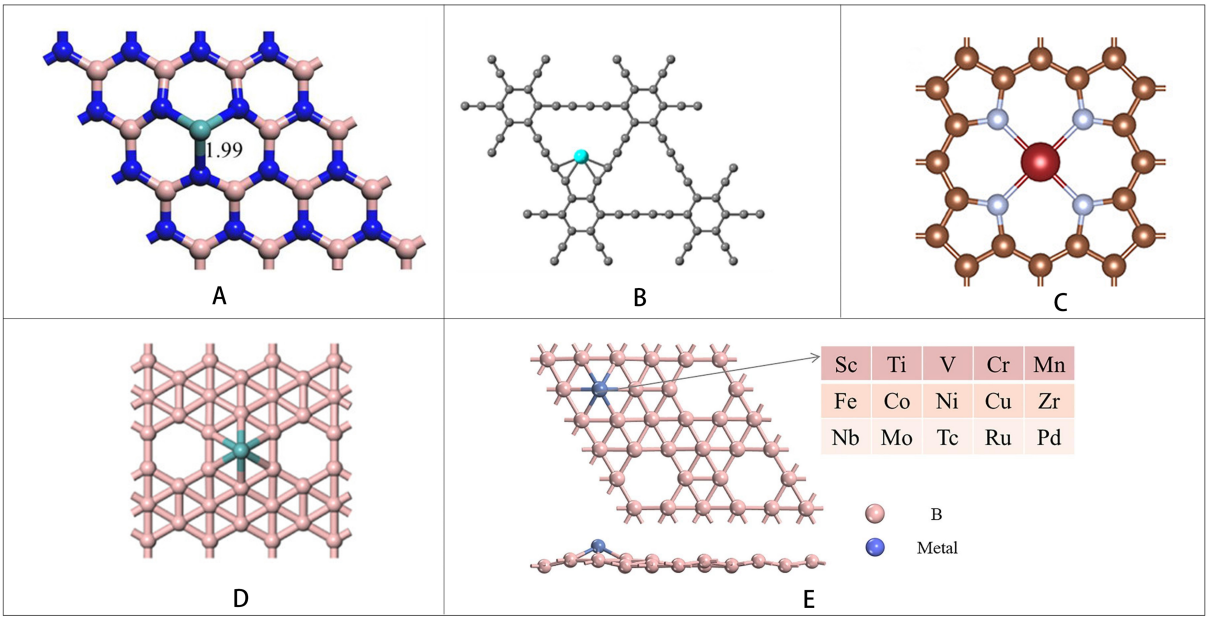

Figure 3. Representative optimized structures of Mo-embedded SACs. (A) Mo-BN, reprinted with permission from Ref.[32]. Copyright © 2017 American Chemical Society; (B) Mo@GDY, reprinted with permission from Ref.[35]. Copyright © 2019 Elsevier B.V.; (C) Mo-Pp, reprinted with permission from Ref.[36]. Copyright © 2020 American Chemical Society; (D) Mo@BM-β_{12}, reprinted with permission from Ref.[37]. Copyright © 2021 American Chemical Society; (E) Mo@BM-α, reprinted with permission from Ref.[38]. Copyright © 2022 Elsevier B.V. SACs: Single-atom catalysts; Mo@GDY: graphdiyne monolayer.

Based on the experimental work by Osuka *et al.* on the tetrameric porphyrin sheet and linear conjugated Zn-Pp tapes[61,62], Liu *et al.* investigated extended 2D TM porphyrin sheets (TM-Pp, TM = Sc, Ti, V, Cr, Mn, Fe, Co, Ni, Cu, Zn, Nb, Mo, Ru) for NRR[36]. Their study indicated that Mo-Pp [Figure 3C] is a promising NRR electrocatalyst under ambient conditions due to its high thermodynamic stability and low U_L.

The combination of edge fluoridation with Mo dopants endowed Mo single atoms anchored on zigzag graphene nanoribbons with H/F terminations (Mo-g/H and Mo-g/F) with excellent NRR properties. Electronic analysis showed that edge termination modulates the binding strength of Mo anchoring, alternating its affinity for NRR intermediates and boosting NRR selectivity[63].

Xu *et al.* systematically studied the NRR activity of metal-atom-embedded M@BM-β_{12} (including 3*d*/4*d* TMs and main group metals) SACs, and their results showed that Mo@BM-β_{12} [Figure 3D] and Mn@BM-β_{12} demonstrate promising properties with U_L of -0.26 and -0.32 V, respectively, and could effectively suppress the competitive hydrogen evolution reaction (HER)[37].

Similarly, Li *et al.* studied the donor-acceptor interaction between TM atoms and N_2, showing that during N_2 activation, the antibonding orbital of N_2 accumulates significant negative charge transferred from the TM atom, thus facilitating the activation of N_2. Among the 20 TMs (3*d*/4*d* TMs) on an α-borobenzene monolayer (BM-α), V@BM-α and Mo@BM-α [Figure 3E] showed the best activity, with U_L of -0.22 and -0.32 V, respectively[38].

Single TM atoms coordinated by N atoms (TM-N_x) are also attractive for NRR. Wang *et al.* reported that the experimentally realized single Mo atoms supported on N-doped carbon (Mo_1-N_1C_2, a Mo atom coordinated by one N atom and two C atoms) exhibited excellent NRR activity *via* the enzymatic

mechanism[39]. Yang *et al.* reported that a single Mo atom supported on nitrogen-doped graphene (Mo_1/Gr_1-N_3G) has high activity and selectivity with low U_L (-0.50/-0.75 V) and high selectivity (40%/100%) *via* a new distal-to-alternating hybrid mechanism involving two spectator N_2 molecules[40].

Liu *et al.* demonstrated that defective graphene substrates could act as electron reservoirs during the NRR process[41]. In a series of single TM atom anchored divacancy 555-777 graphene systems (containing three pentagons and three heptagons constructed by removing two neighboring C atoms), MoN_3@555-777 graphene sheets showed good catalytic activity with a low U_L of -0.57 V.

Niu *et al.* explored a series of TM atoms (from Sc to Au) supported on graphitic carbon nitride (*g*-CN) SACs for NRR[42]. Due to high activity (with low U_L of -0.42, -0.39, -0.35, -0.29, and -0.39 V, respectively), high selectivity (100%, 100%, 100%, 94%, and 69%, respectively), and good kinetic stability, Nb, Mo, Ta, W, and Re/*g*-CN were identified as efficient NRR electrocatalysts.

In summary, leveraging the advantages of Mo atom active centers inspired by natural nitrogenase and 2D substrate materials holds great promise for achieving the catalytic conversion of N_2 to NH_3 under mild conditions. This can be realized by precisely tuning the coordination environment of Mo atoms. Furthermore, a detailed and accurate characterization of the electronic structure of SACs is essential for gaining a deeper understanding of their NRR activity[64].

Non-Mo-based SACs

Fe-based SACs

Apart from Mo, Fe has garnered significant attention as an essential metal in nitrogenase enzymes responsible for biological nitrogen fixation[65]. For example, Fe-based catalysts have been widely used in the industrial Haber-Bosch process for NH_3 synthesis[66]. Li *et al.* demonstrated that a highly spin-polarized FeN_3 active center on graphene with a local magnetic moment, which enhances N_2 adsorption and activation, is a promising NRR catalyst at room temperature[67]. Li *et al.* revealed that Fe(V)-PTC exhibited excellent NRR activity among a series of TM-PTC (TM = Fe, Sc, Ti, V, Cr, Mn, Co, Ni, Cu) SACs, attributed to the donation/back-donation mechanism[68]. Sahoo *et al.* investigated the NRR mechanism for single Au and Fe atoms supported on C_2N monolayers. Their findings indicated that Fe-C_2N was a better catalyst than Au-C_2N, with a U_L of -0.7 V, owing to its stronger N_2 adsorption energy[55].

V-based SACs

Vanadium nitrogenase is another biological nitrogenase system in nature[69]. Therefore, researchers have extensively studied the NRR performance of V-based SACs.

Among others, Choi *et al.* examined the NRR performance of single atoms anchored on defective graphene derivatives by DFT computations[56]. Ti@N_4 and V@N_4 were identified as efficient catalysts with low U_L and high selectivity due to strong back-bonding interactions between the hybridized *d*-orbital metal atoms and the π^* orbital of $^*N_2$. Zhu *et al.* found that V/β_{12}-BM demonstrated good energy efficiency for NRR due to the acceptor-donor interaction between the V atom and N_2[57].

Zhen *et al.* showed that TM@GDY nanomaterials (TM = Ti, V, Fe, Co, Zn, Rh, Hf) are promising SACs for NRR, surpassing Ru(0001) stepped surfaces in performance. In particular, V@GDY exhibited the lowest U_L of -0.67 V[58]. Most recently, Xu *et al.* screened V-, Fe-, Co-, and Ru-doped arsenene nanosheets, identifying them as efficient, low-cost NRR catalysts. In particular, during the NRR process, the arsenene nanosheet acts as a medium for accepting and donating electrons, while VAs_3 serves as a charging transmitter between

N_xH_y species and the nanosheet, resulting in high catalytic efficiency for V-doped arsenide (V/Ars) with a low U_L of -0.26 V[59].

The study of bio-inspired catalysts with Mo-, Fe-, and V-like nitrogenase active centers for ammonia synthesis at room temperature and atmospheric pressure holds great potential but presents significant challenges. Much work remains to be done, particularly concerning the underlying mechanisms.

Nobel metal-based SACs

Noble metal-based catalysts, such as Ru and Pt, have been extensively studied for NRR due to their strong electron-donating properties, which arise from their unfilled *d* orbitals.

Liu *et al.* proposed that single Ru atoms anchored in hexagonal pores of boron monolayers (Ru/B α-sheet and Ru/B β_{12}-sheet) could serve as promising monoatomic NRR catalysts, with reaction energy barriers less than half that of flat Ru(0001) catalysts[70]. Yin *et al.* found that Pt/*g*-C_3N_4 exhibited outstanding NRR catalytic activity at room temperature, with a low U_L of -0.24 V, attributed to the synergistic interaction between Pt atoms and the *g*-C_3N_4 substrate, which optimized the energetics of $^*N_2H$ and $^*NH_2$ intermediates[71].

SACs with other TMs

While noble metal catalysts have shown promise for NRR, their high cost limits their large-scale application. TMs, such as W, Co, Nb, and Ni, are also being considered as active centers for NRR.

Chen *et al.* evaluated the catalytic performance of a series of single metal atoms loaded on *g*-C_3N_4[72]. The NRR catalytic activity of five TMs (Ti, Co, Mo, W, and Pt) supported on *g*-C_3N_4 monolayers exceeded that of Ru(0001) stepped surfaces. W@ *g*-C_3N_4, in particular, showed the highest catalytic activity with a U_L of -0.35 V, attributed to the significant positive charge and large spin moment on the W atom, resulting in a moderate adsorption strength for NRR intermediates.

Wang *et al.* studied the NRR behavior of SACs formed by a series of single TM atoms (from Sc to Zn) anchored on *g*-C_9N_{10}. They found that Mn/*g*-C_9N_{10} exhibited excellent NRR activity with a low U_L of -0.295 V through the distal pathway[73]. Saeidi *et al.* reported that Co/N_3-Gr (Co atoms incorporated into N-modified graphene) is a promising NRR catalyst with lower energy consumption and better stability, preferring the alternating associative pathway with a U_L of -0.53 eV[74].

The Ni@Ti_2NO_2 MXene structure, which satisfies orbital symmetry matching, could achieve an acceptor-donor interaction, allowing N_2 to be transformed *via* a novel "enzyme-distal" mechanism due to the synergistic interaction between Ti and Ni atoms[24].

Additionally, Nb and W embedded in defective boron phosphide (BP) monolayers with boron monovacancies (Nb/BP and W/BP) were documented as promising NRR electrocatalysts with low U_L (-0.25 and -0.19 V), attributed to the favorable matching between the *d*-orbitals of Nb or W atoms and the *p*-orbitals of the N_2 molecule above the Fermi level (E_F)[75].

Gao *et al.* reported a theory-guided design of Nb catalysts supported on anatase TiO_2(110) for NRR. Theoretical calculations showed that dispersing Nb atoms on anatase TiO_2(110) significantly increased electron density at the E_F, enhancing conductivity and facilitating the proton-coupled electron transfer process, thus leading to excellent NRR activity and selectivity for Nb-TiO_2(110)[76].

Importance of coordination environment

Non-noble metal catalysts are advantageous due to their low cost and abundant availability; however, they often have weaker electron-donating abilities compared to noble metals. To enhance electron donation, heteroatoms are often introduced to regulate the density of *d*-orbital states[77]. At present, it remains a significant challenge to select matched heteroatoms to regulate the structure of non-noble metal catalysts accurately.

Zhao *et al.* recently proposed that introducing boron dopants in Fe-N_4/G could effectively regulate the interaction between active centers and $^*N_2H$ species. Specifically, Fe coordinated by two boron and two nitrogen atoms exhibited outstanding NRR activity[78]. Wang *et al.* studied TM atoms anchored on N/O-codoped graphene (TM-O_xN_y@Gra, $x + y = 4$) for NRR, demonstrating that catalytic performance can be modulated through coordination engineering[79]. Tang *et al.* identified two excellent NRR catalysts (V-S_2C@Cr and V-S_3@Cr) by doping sulfur atoms in the coordination environment of V from over eight SACs (V-S_xC_{NC-x}@Cr)[80].

These results indicate that, in addition to TM active centers, the coordination environment plays a crucial role in catalytic activity. Synergistic effects can modify electronic structures, thereby creating a favorable environment for nitrogen fixation, promoting chemisorption of N_2 molecules, and activating the inert N≡N triple bond. Furthermore, the prediction of the catalytic activity of each SAC should be complemented by parallel investigations into its stability[81].

To facilitate comparison of catalytic performance, the reaction mechanisms and U_L of various catalysts are summarized in Table 2.

SCCS TOWARDS NRR

In recent years, SCCs for NRR have garnered significant research interest. While catalytic processes are often simplified into reactant adsorption and product desorption, a deeper understanding of the catalytic enhancement of SCCs can emerge from analyzing the synergistic interactions within atomic clusters and between clusters and substrates. Moreover, the flexible clusters can adaptively modify their structure during the reaction process, thereby significantly improving their catalytic activity[87]. In this subsection, we will focus on three kinds of SCCs: DACs, TACs, and transition metal-free catalysts (TMFCs).

DACs

Compared to SACs, DACs offer multiple active sites, enabling diverse adsorption modes [Figure 4A][88]. The reactivity and activation mechanisms of SACs and DACs may also be different due to distinct *d*-orbital occupations - σ-donation/π-backdonation for SACs and π-donation/π-backdonation for DACs [Figure 4B][89].

DACs can modify the adsorption and activation modes of reactants, intermediates, and products through the synergistic interactions between multiple atomic sites, thereby enhancing the reactivity. For example, varying N_2 adsorption configurations on Mn@C_2N and Mn_2@C_2N lead to greater charge transfer from the Mn's *d* orbitals to N_2's antibonding orbitals in the Mn_2@C_2N system, resulting in higher NRR activity [Figure 4C][90]. However, further development of catalytic systems with multiple active sites remains essential to enhance activity, stability, and selectivity.

Homonuclear metal dimers anchored on 2D substrates have demonstrated superior NRR performance compared to their single-atom counterparts, such as Cr_2-N_6G and Mn_2-N_6G[22], Cr_2@C_2N and V_2@C_2N[89],

Table 2. Summary of the metal atoms other than Mo/Fe/V-based SACs towards NRR

System	Limiting potential/V	Reaction mechanism	Year of publication
Ni@Ti_2NO_2	-0.13	Enzymatic-distal	2021[24]
Mn@BM-β_{12}	-0.32	Distal	2021[37]
Ta@BM-β_{12}	-0.38	Enzymatic	
Cr@BM-β_{12}	-0.48	Enzymatic	
V@BM-α	-0.22	Enzymatic	2022[38]
Gr_1/N_3-G	-0.75	Distal-to-alternating hybrid	2019[40]
Nb/*g*-CN	-0.42	Distal	2020[42]
Ta/*g*-CN	-0.35	Distal	
W/*g*-CN	-0.29	Distal	
Re/*g*-CN	-0.39	Distal	
Ru/CeO_2-S	-0.35	Distal	2019[48]
Ta@BN	-0.59	Enzymatic	2020[52]
Ti@*g*-C_3N_4	-0.84	Alternating	2023[54]
Ru/B α-sheet	-0.58	Distal	2019[70]
Ru/B β_{12}-sheet	-0.60	Distal	
Pt/*g*-C_3N_4	-0.24	Alternating	2019[71]
W@*g*-C_3N_4	-0.35	Enzymatic	2018[72]
Mn/g-C_9N_{10}	-0.295	Distal	2023[73]
Co/N_3-Gr	-0.53	Enzymatic	2019[74]
Nb/BP	-0.25	Enzymatic	2021[75]
W/BP	-0.19	Enzymatic	
Fe–B_2N_2/G	-0.65	Distal	2021[78]
V-N_4@Gra	-0.44	Consecutive	2022[79]
Ta-N_4@Gra	-0.49	Distal	
V-O_1N_3@Gra	-0.40	Consecutive	
V-$O_2N_2^{\alpha}$@Gra	-0.42	Consecutive	
V-$O_2N_2^{\beta}$@Gra	-0.44	Consecutive	
V-$O_2N_2^{\gamma}$@Gra	-0.38	Consecutive	
V-O_3N_1@Gra	-0.39	Consecutive	
Mo-O_3N_1@Gra	-0.48	Distal	
V-O_4@Gra	-0.43	Consecutive	
Ru-O_4@Gra	-0.43	Distal	
V-S_3@Gr	-0.00	Mixed	2023[80]
V-S_2C@Gr	-0.17	Mixed	
Ti@CN	-0.38	Enzymatic	2021[82]
Nb@P_3-Ars	-0.52	Distal	2021[83]
Ta@*g*-C_7N_3	-0.27	Distal	2022[84]
W@*g*-C_7N_3	-0.06	Alternating	
Mn@GY	-0.36	Distal	2021[85]
U@N_1C_2	-0.46	Enzymatic	2022[86]
		Consecutive	

SACs: Single-atom catalysts; NRR: nitrogen reduction reaction; BM-β_{12}: metal-doped β-borophene; BM-α: metal-doped α-borophene; N_3-G: N-doped graphene; *g*-CN: graphitic carbon nitride with the CN stoichiometric ratio; CeO_2-S: stepped CeO_2; BN: hexagonal boron nitride; *g*-C_3N_4: graphitic carbon nitride with the C_3N_4 stoichiometric ratio; B α-sheet: boron α-sheet; B β-sheet: boron β-sheet; g-C_9N_{10}: graphitic carbon nitride with the C_9N_{10} stoichiometric ratio; N_3-Gr: N-doped graphene; BP: defective boron phosphide monolayer with B-monovacancy; Fe-B_2N_2/G: B doped Fe-N-C catalysts; TM-O_xN_y@Gra: transition metals anchored on N/O-codoped graphene; V-S_3@Gr: V-archored S-doped graphene; CN: graphitic carbon nitride with the CN stoichiometric ratio; P_3-Ars: P_3-doped defective arsenene; C_7N_3: graphitic carbon nitride with the C_7N_3 stoichiometric ratio; GY: graphyne; U@N_1C_2: U-archored nitrogen-carbon based catalysts.

Mo_2@C_2N[91], and binuclear Mo on N-doped nanoporous graphene (Mo_2-N-C)[92]. Recently, Zhang *et al.* revealed that the presence of a second metal atom not only modulates the electronic structure but also

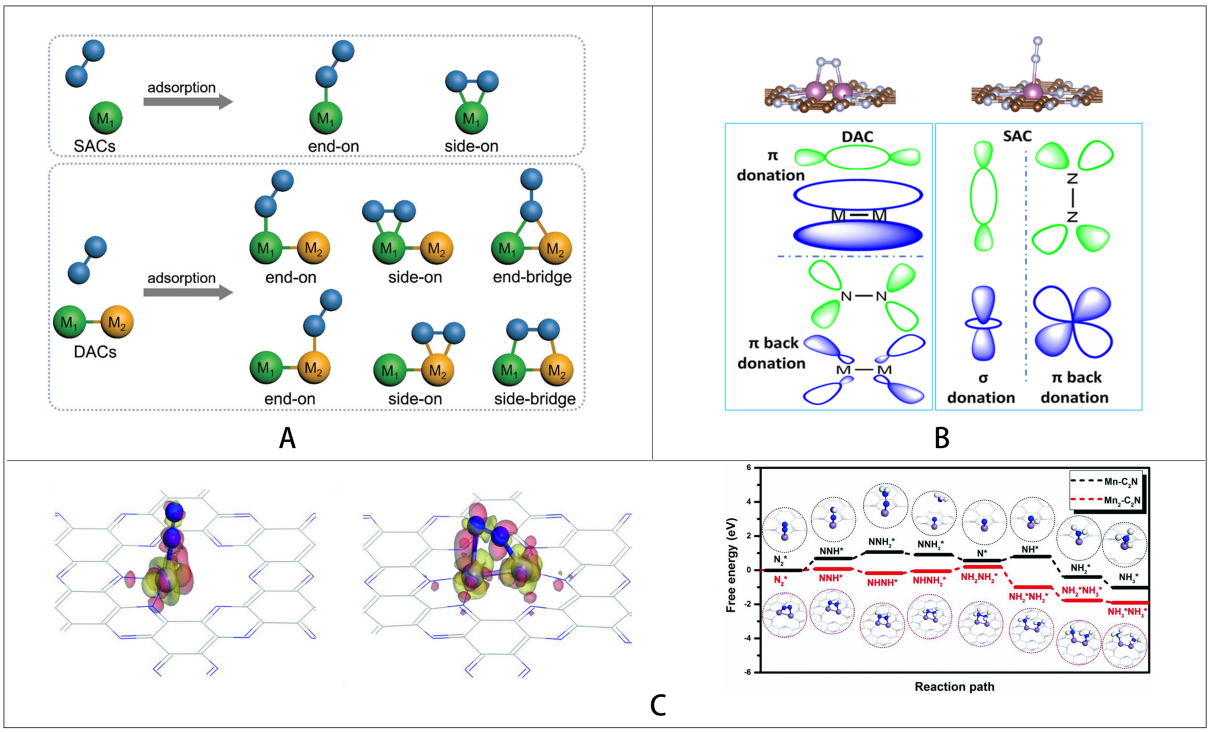

Figure 4. (A) Schematic diagram of adsorption configurations of diatomic molecules at single-atom site and dual-atom site. Reprinted with permission from Ref.[88]. Copyright © 2022 Wiley-VCH GmbH; (B) N_2 molecule activation mechanism for the SACs and DACs. Reprinted with permission from Ref.[89]. Copyright © 2020 The Authors. EcoMat published by John Wiley & Sons Australia; (C) Adsorption configuration and corresponding charge density difference of N_2 and free energy diagrams of NRR on $Mn@C_2N$ and $Mn_2@C_2N$. Reprinted with permission from Ref.[90]. Copyright © 2019 Wiley-VCH Verlag GmbH & Co. KGaA, Weinheim. SACs: Single-atom catalysts; DACs: diatomic catalysts; NRR: nitrogen reduction reaction.

actively participates in N_2 activation and early hydrogenation through a unique N_2 adsorption configuration. This configuration disrupts the undesirable linear scaling relationships of key intermediate adsorption energies on the catalyst surface. The effective cooperation of dimers resulted in excellent NRR performance, as demonstrated by $V_2@g\text{-}C_3N_4$ and $Ni_2@g\text{-}C_3N_4$ [Figure 5A][93,94].

Furthermore, heteronuclear metal dimers in the DACs may exhibit even better performance than homonuclear dimers due to the *d*-orbital electronic structure modulation enabled by heteronuclear atom synergy[95]. Recent examples include Fe/Mn-N-C[96], Mo-Ru, Mo-Co, Mo-W, Mo-Fe, and Fe-Ru embedded in a nitrogen-doped graphene framework[97], FeMo@NG[98], $CoMo@N_6$[99], FeCo@GDY and NiCo@GD[100]. Yang *et al.* recently proposed a novel N_2 activation strategy, showing that the reactivity of X/Fe-N-C (X = Pd, Ir, Pt) dual-atom catalysts for N_2 reduction can be adjusted by local hydrogen radical (H^*) on the X site [Figure 5B][94]. These findings reinforce that DACs can surpass SACs in NRR performance, driven by the tailored *d* stated electronic structure resulting from the metal dimer synergy.

TACs

Compared to the synthesis of DACs, preparing TACs is more challenging because it is difficult to control the number of atoms during synthesis precisely. Additionally, the high surface energy of low-coordinate atoms in TACs necessitates the use of an appropriate substrate to improve stability. The adsorption configuration of N_2 on TACs is also more complex than that on DACs [Figure 6A], and research into TACs is still in its infancy[101]. In the following sections, we will explore some of their applications in NRR.

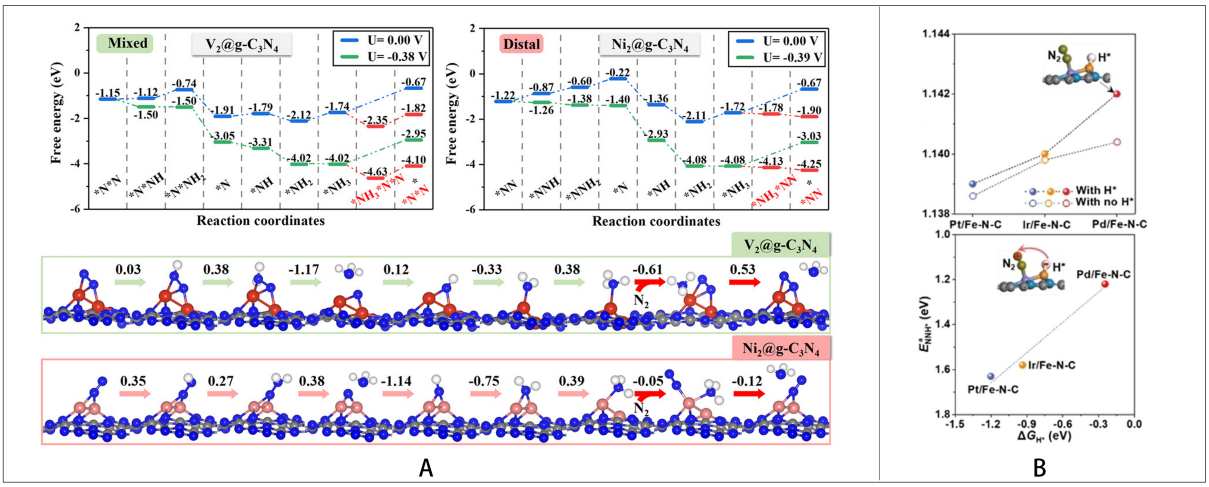

Figure 5. (A) Free energy profiles and corresponding intermediate structures on V_2@g-C_3N_4 andNi_2@g-C_3N_4, Color scheme: H, white; C, gray; N, blue; V, red; Ni, pink. Reprinted with permission from Ref.[93]. Copyright © 2022 Wiley-VCH GmbH; (B) N≡N bond lengths with and without H* generated on the X site and the relationship between G_{H^*} and $E^a_{NNH^*}$ on X/Fe-N-C (X = Pd, Ir, Pt), with an inset showing the schematic diagram of the cleavage of X–H bond to form NNH*. Reprinted with permission from Ref.[94]. Copyright © 2023 Wiley-VCH GmbH.

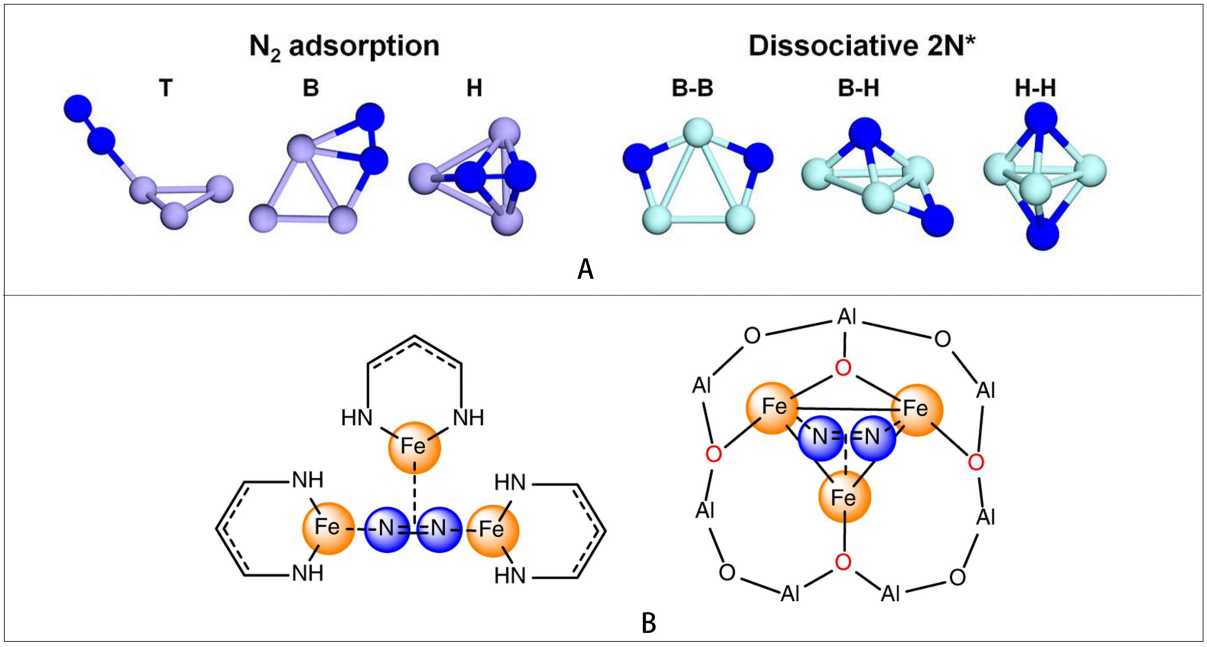

Figure 6. (A) Adsorption and dissociative adsorption structures of N_2 on three-metal clusters. Reprinted with permission from Ref.[101]. Copyright © 2022 American Chemical Society; (B) Homogeneous and heterogeneous Fe_3 cluster with N_2 adsorption. Reprinted with permission from Ref.[102]. Copyright © 2018, The Author(s).

Liu et *al.* proposed a Fe_3 cluster catalyst anchored on the surface of θ-Al_2O_3 (010) [Figure 6B] based on first-principles calculations and micro-kinetic analysis. The electron interaction between the Fe clusters and the substrate was very weak, resulting in a very low oxidation state for Fe atoms within the metal-metal bonded Fe_3 clusters. Notably, these low oxidation state Fe_3 clusters can serve as electron reservoirs, dynamically adjusting charge in the reaction process. In addition, the significant spin polarization of Fe atoms was identified as a critical factor in facilitating N_2 activation[102].

Chen *et al.* investigated the NRR activity of SACs, DACs, and TACs supported on heterogeneous graphylene and graphene, denoted as M_x-GDY/Gra (where M = Mn, Fe, Co, and Ni; x = 1, 2, 3). Their findings showed that TACs exhibited better stability and catalytic performance than SACs and DACs, with Fe_3-GDY/Gra with a theoretical mass loading of 35.8 wt% achieving a particularly low U_L of -0.26 V. This enhanced activity was attributed to the M_3 active site, which not only provided additional electrons for N_2 activation but also displayed weaker adsorption of the product, facilitating easier release[103].

The reaction mechanisms and U_L of DACs and TACs are summarized in Table 3; however, TACs are not always superior to DACs. Luo *et al.* demonstrated that Fe_2/MoS_2 exhibits high catalytic activity for NRR. Their findings suggest that, compared to Fe/MoS_2, the presence of adjacent Fe atoms in Fe_2/MoS_2 enables a side-on adsorption configuration for N_2, which is more favorable for effective activation. However, the addition of a third Fe atom (Fe_3/MoS_2) reduces electron sharing between Fe atoms, thereby inhibiting N_2 adsorption[110].

In summary, the factors influencing NRR activity and selectivity are complex, and the catalytic performance of multi-atom clusters in NRR depends on the specific atomic configuration. Further research is needed to understand the underlying characteristics.

TMFCs

TMFCs, such as boron-based catalysts, have shown promise for the NRR. Due to the sp^3 or sp^2 electron configuration, boron atoms can provide empty orbitals that facilitate N_2 activation. For example, Anis *et al.* investigated single, double, and triple boron atoms supported on a GDY monolayer (B@GDY, B_2@GDY, and B_3@GDY) for NRR, concluding that B_3@GDY demonstrates outstanding catalytic performance and effectively suppresses HER [Figure 7A][111]. Similarly, Wang *et al.* proposed that a g-C_3N_4 monolayer embedded with double B atoms (B_2@C_3N_4) enhances N_2 activation [Figure 7B]. Their findings suggest strong hybridization between N_2-2p orbitals and B-sp^3 orbitals, which accounts for the high catalytic efficiency of B_2@C_3N_4[112]. In a related study, Rasool *et al.* explored NRR on single- and double-boron-doped configurations across five different substrates, demonstrating that g-C_3N_4 is particularly effective[113].

These studies highlight boron-based TMFCs as efficient and selective NRR catalysts, offering a viable alternative to TMs by utilizing unique electronic interactions that enhance N_2 activation while suppressing HER. This approach broadens the materials landscape for sustainable, TM-free catalysis. More efforts are encouraged to explore such catalysts, especially with elements beyond boron.

HIGH-THROUGHPUT CALCULATIONS AND EMERGING MACHINE LEARNING TOWARDS NRR

The search for materials with specific properties is challenging, as traditional trial-and-error methods are often inefficient. However, combining high-throughput computing with machine learning (ML) offers a powerful approach for materials prediction and design, addressing long development cycles and high costs, and accelerating the discovery of novel catalysts[114].

High-throughput DFT calculations

TM elements, coordination environments, and substrates significantly influence NRR efficiency, and the numerous possible combinations can greatly benefit from high-throughput DFT calculations to streamline the search for optimal configurations[115].

Table 3. Summary of the DACs and TACs towards NRR

Systems	Limiting potential/V	Reaction mechanism	Year of publication
$Mo_2@C_2N$	-0.35	Enzymatic	2018[91]
$V_2@g\text{-}C_3N_4$	-0.38	Mixed	2022[93]
$Ni_2@g\text{-}C_3N_4$	-0.39	Distal	
TiV@BP	-0.38	Mixed	2023[95]
TiCo@BP	-0.31	Distal	
VCr@BP	-0.41	Distal	
VCo@BP	-0.31	Distal	
VNi@BP	-0.38		
Fe/Mn-N-C	-0.37	Distal	2020[96]
Mo-RuN_6-NG	-0.17	Enzymatic	2020[97]
Mo-CoN_6-NG	-0.27	Enzymatic	
Mo-WN_6-NG	-0.28	Distal	
Mo-FeN_6-NG	-0.36	Enzymatic	
Fe-RuN_6-NG	-0.39	Enzymatic	
$CoMo@N_6$	-0.52	Distal	2020[99]
FeCo@GDY	-0.44	Distal	2021[100]
NiCo@GDY	-0.36	Distal	
Fe_3-GDY/Gra	-0.26	Distal	2020[103]
$Mo_2@B_2\text{-}C_2N$	-0.25	Enzymatic	2024[104]
$Fe_3@C_2N$	-0.57	Enzymatic	2020[105]
$Fe_3@N_4C_6$	-0.45	Enzymatic	2023[106]
VNiCu@NV-W_2N_3	-0.05	Enzymatic	2023[107]
Fe_2Co@NV-W_2N_3	-0.49	Enzymatic	
Fe_3@NV-W_2N_3	-0.10	Enzymatic	
$Pt_3@C_3N_3$	-0.24	Enzymatic	2023[108]
$Ru_3@C_3N_3$	-0.35		
$Ru_3@g\text{-}C_3N_4$	-0.19	Enzymatic	2024[109]
$Rh_3@g\text{-}C_3N_4$	-0.02	Enzymatic	

DACs: Diatomic catalysts; TACs: triatomic catalysts; NRR: nitrogen reduction reaction; BP: black phosphorus; Fe/Mn-N-C: Fe and Mn embedded in N-doped graphene; NG: N-doped graphene; GDY: graphdiyne.

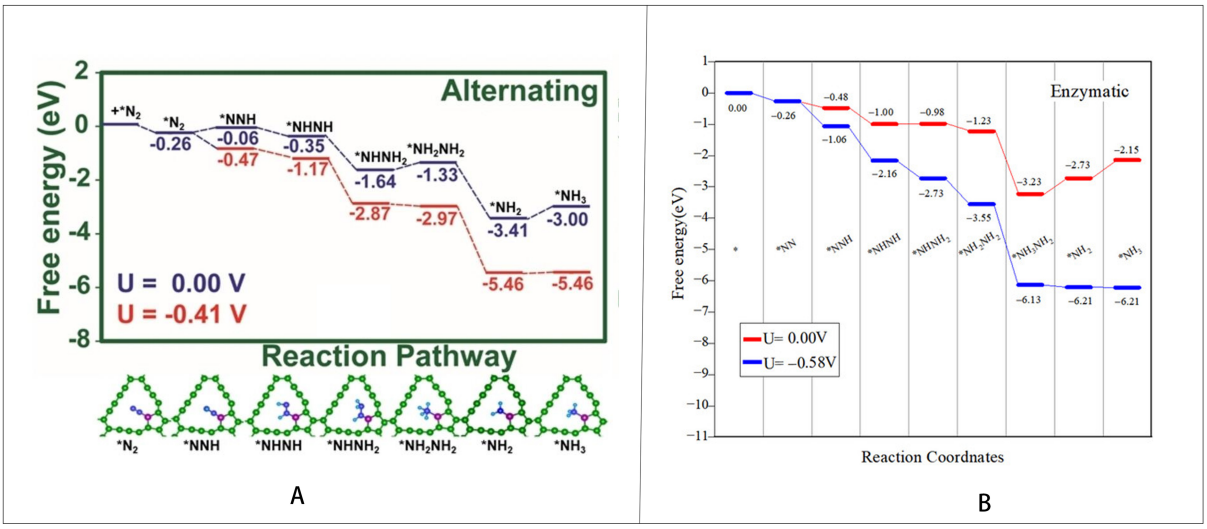

Figure 7. (A) Free energy profiles and the optimized geometries of reaction intermediates for the NRR on B_3@GDY. Reprinted with permission from Ref.[111]. Copyright © 2023 Wiley-VCH GmbH; (B) Free energy profiles for the NRR on $B_2@C_3N_4$. Reprinted with permission from Ref.[112]. Copyright © 2022 by the authors. NRR: Nitrogen reduction reaction; GDY: graphdiyne.

By exploring extensive combinations, researchers can more effectively identify catalysts with promising

properties for NRR applications. Lv *et al.* developed a "five-step" screening strategy [Figure 8A] using high-throughput DFT calculations to evaluate TM_2/CN catalysts for NRR. This approach identified Fe_2/g-CN as a highly active catalyst with low energy consumption and high selectivity, concluding that moderate electron donation from TM to N_2 is crucial for balancing N_2 activation and $^*NH_3$ formation steps[116]. Similarly, Sun *et al.* used high-throughput computations to screen $TM_1TM_2@C_9N_4$ [TM_1, TM_2 = 3(4) *d* TM atoms] and identified five effective catalysts (TM_1, TM_2 = NiRu, FeNi, TiFe, TiNi, NiZr) with strong activity[117]. Sun *et al.* further applied a "four-step" screening strategy [Figure 8B], predicting that six catalysts, including $W@V_B$-V_1-BC_3, $Re@V_B$-V_1-BC_3, $Mo@V_B$-V_2-BC_3, $Ti@V_B$-V_3-BC_3, $Mo@V_B$-V_3-BC_3, and $Ta@V_C$-V_1-BC_3, exhibited superior NRR activity and selectivity out of 33 candidates[118]. Pei *et al.* systematically assessed the stability of 3*d*-5*d* TM trimers embedded in C_3N_3 nanosheets ($TM_3@C_3N_3$) and found that configurations with Re, Ru, or Pt trimers demonstrated excellent catalytic activity for NRR[108].

ML

While high-throughput computing provides a structured approach for catalyst design, the massive data generated can obscure key performance factors, making it challenging to pinpoint the critical influences on catalytic performance. Advanced data analysis tools are crucial to fully leverage high-throughput screening for next-generation NRR catalysts. Emerging ML techniques are providing us with such a solution, enabling rapid and efficient data extraction, prediction, and analysis. By accelerating the identification of high-performance materials from thousands of candidates, ML not only enhances our understanding of structure-activity relationships but also sheds light on the fundamental mechanisms of catalysis [Figure 9A][118].

In recent years, ML has shown promise in catalyst design, with applications emerging in NRR research. Wang *et al.* used ML techniques to explore the nitrogen reduction reactivity of novel, graphene-supported SACs, based on their prior high-throughput calculations [Figure 9B]. Their study evaluated 29 TMs and 57 ligand structures, generating 1,626 unexplored catalyst configurations. Using a trained ML model, they predicted four target properties (E_f, ΔE_{N_2}, $\Delta G_{N_2\text{-}N_2H}$, $\Delta G_{NH_2\text{-}NH_3}$) of these configurations and identified 45 promising candidates for NRR [Figure 9C]. Among these, Mo-B_2CN-(orthogonal-B) performs the best, with exceptionally low free energy along the distal pathway. Through statistical analysis, the researchers developed a predictive descriptor (ΔE_{N_2}, $\Delta G_{N_2\text{-}N_2H}$, $\Delta G_{NH_2\text{-}NH_3}$) with high generalizability, applicable to untested NRR catalyst systems[119].

Zhang *et al.* also applied ML models to evaluate the catalytic activity of SACs by directly predicting reaction Gibbs free energy. Their findings underscored the high predictive accuracy of the gradient boosting regression (GBR) model for both ΔG ($^*N_2 \rightarrow {}^*NNH$) and ΔG ($^*NH_2 \rightarrow {}^*NH_3$). Feature importance analysis revealed that the accuracy of the GBR model was due to its effective identification of key characteristics related to the active center and coordination environment, with the covalent radius emerging as a particularly influential descriptor[120].

Despite its potential, ML-based catalyst selection is currently constrained by limited experimental data. Nevertheless, integrating high-throughput screening with ML strategies offers a promising pathway for catalyst discovery, opening new horizons for efficient and targeted materials design.

DESCRIPTOR-BASED SCREENING AND DESIGN OF NRR CATALYSTS

Given the complexity of multiple intermediates in the NRR process, developing simplified parameters for evaluating catalyst activity is beneficial. Compared with heavy DFT computations, descriptors can quickly predict catalyst performance, providing experimental researchers with a practical tool for screening high-

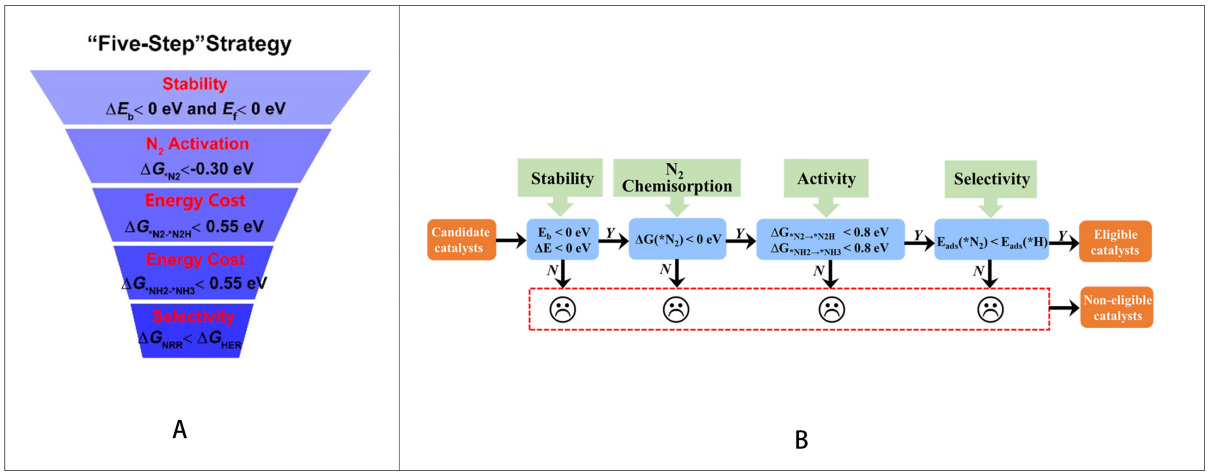

Figure 8. (A) "Five-step" screening strategy. Reprinted with permission from Ref.[116]. Copyright © 2021 American Chemical Society; (B) "Four-step" screening strategy. Reprinted with permission from Ref.[118]. Copyright © 2023 The Authors. Energy & Environmental Materials published by John Wiley & Sons Australia, Ltd on behalf of Zhengzhou University.

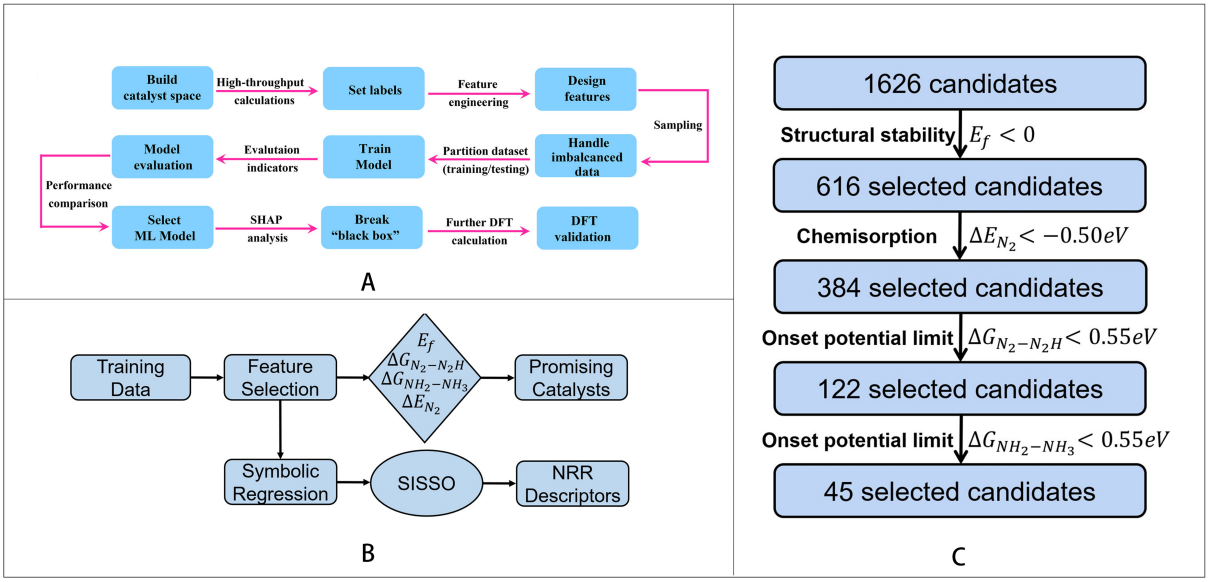

Figure 9. (A) The workflow of ML to explore the origins of catalysis. Reprinted with permission from Ref.[118]. Copyright © 2023 The Authors. Energy & Environmental Materials published by John Wiley & Sons Australia, Ltd on behalf of Zhengzhou University; (B) ML screening and descriptor building framework of the work by Zhang *et al.*; (C) Workflow of the ML screening process as well as the number of selected candidates after each screening step of the work by Zhang *et al.* Reprinted with permission from Ref.[119]. Copyright © 2021 Zhengzhou University. ML: Machine learning.

performance materials. By identifying trends in electrocatalytic properties and using reactivity descriptors to forecast promising catalysts, we can realize the rational design of catalysts, especially for processes as complicated as NRR.

Adsorption energy descriptors

The adsorption energy reflects the strength of the interaction between the reactant and the catalyst and is a key indicator for selecting high-efficiency catalysts. When the adsorption energy falls within the optimal range, it reduces the reaction energy barrier and, consequently, the U_L. Catalysts with moderate adsorption

energy generally exhibit lower U_L, making adsorption energy a simple and effective descriptor.

Chen *et al.* demonstrated that the NRR activity of TM/MoS_2 catalysts is affected by the *d*-orbital electron density states at the E_F, with N_2 adsorption inversely proportional to the U_L value[121]. Similarly, Ma *et al.* investigated the activity of TM (TM = Mn, Fe, Co, Ni)-based SACs/DACs/TACs on GDY, finding an approximate linear relationship between the adsorption energy of $^*N$ and U_L[122].

Considering that the formation of $^*N_2H$ is the potential determining step, Ren *et al.* examined the scaling relation between the adsorption energy of $^*N_2H$ and U_L, concluding that Nb atoms supported on *g*-C_3N_4 are particularly promising NRR catalysts due to their low U_L and strong N_2H^* adsorption[123]. Luo *et al.* further observed that $^*N_2H$ and $^*NH_2$ adsorption energies are proportional to $\Delta E(^*N)$ on TM-modified Co_4 clusters supported on GDY, revealing the scaling relationship among the adsorbed N_xH_y species. They concluded that tightly bound N atoms hinder NH_3 formation, while loosely bound N atoms impede protonation of $^*N_2$ to $^*N_2H$. The results showed that the NRR activity of TM/*g*-CN catalyst can be well estimated by the adsorption energy of $^*N$[124].

Collectively, these findings suggest that adsorption energy is a useful descriptor for estimating NRR activity, despite its limitation as a theoretical measure that lacks experimental control.

Electronic descriptors

The degree of electronic coupling between adsorbed intermediates and the catalyst also plays a central role in catalytic activity[116]. The crystal orbital Hamilton population (COHP) method, grounded in DFT calculations, provides a powerful tool for analyzing the electronic structure of chemical bonds within a crystal. Specifically, it characterizes the bonding and antibonding interactions between atoms. Its integrated counterpart, the integrated COHP (ICOHP), aggregates COHP values over a defined energy range, capturing both bonding and antibonding contributions to offer a holistic measure of bond strength. In NRR, COHP and ICOHP are commonly used to assess bonding and antibonding populations and the interactions between the catalyst and NRR intermediates. These tools provide critical insights into the formation and cleavage of chemical bonds during the reaction, deepening our understanding of the origins of NRR activity.

As shown in Figure 10A, interactions between various TM centers and NRR intermediates can be categorized into bonding states below the E_F and antibonding states above E_F. These unique properties make COHP a powerful and effective electronic descriptor for evaluating catalytic performance.

Through an ICOHP analysis, Niu *et al.* examined the bonding and antibonding states of N_xH_y intermediates adsorbed on TM/g-CN, finding a strong linear correlation (R^2 = 0.84) between ICOHP and $^*N$ adsorption energy [Figure 10B][42]. Similarly, Liu *et al.* applied ICOHP analysis to assess the NRR performance of TM@N_6-G and TM@g-C_2N, revealing a good linear relationship between ICOHP and $\Delta G_{N2\text{-}NNH}$ (R^2 = 0.88 and 0.99, respectively) [Figure 10C and D][125]. These results indicate that ICOHP is a promising descriptor to describe the NRR activity of SACs and SCCs.

In addition to ICOHP, other electronic properties, particularly spin magnetic moment, have been explored as descriptors for NRR. Wang *et al.* investigated the catalytic activity of SACs on 2D VSe_2, finding that the U_L for NRR is linked to the total magnetic moment of TM-VSe_2[126]. Zhang *et al.* further studied dual single-atom sites, discovering that the metal atoms located in adjacent vacancies can regulate the spin magnetic moment of the active Fe atoms despite a large distance, thereby enhancing N_2 activation and reduction[127].

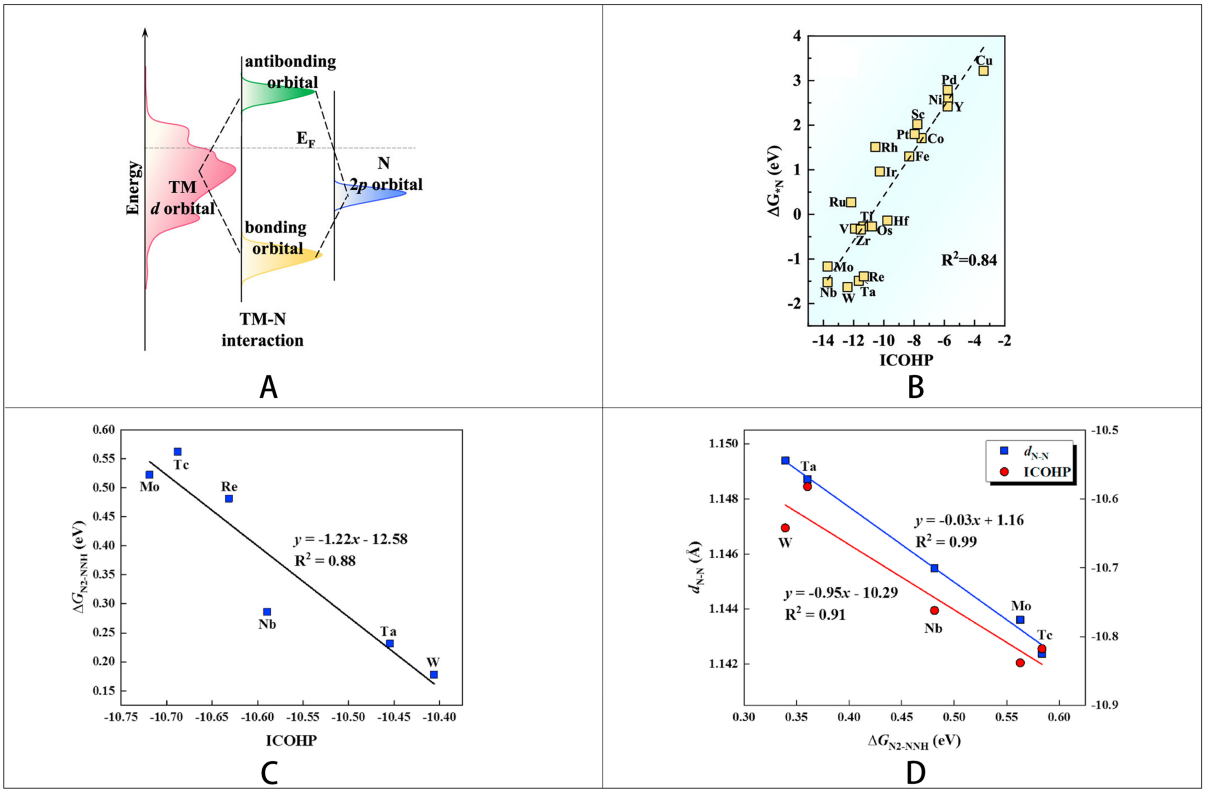

Figure 10. (A) Schematic diagram illustrating how TM centers interact with NRR intermediates (*N as an example) on TM/g-CN; (B) Linear relationship between ICOHP and the adsorption energy of *N on TM/g-CN. Reprinted with permission from Ref.[42]. Copyright © 2020, American Chemical Society; (C) and (D) Linear relationships between ICOHP and $\Delta G_{N2\text{-}NNH}$ on TM@N_6-G and TM@g-C_2N. Reprinted with permission from Ref.[125].Copyright © 2022, Elsevier B. V. TM: Transition metal; NRR: nitrogen reduction reaction; ICOHP: integrated crystal orbital Hamilton population.

Multiple-level descriptors

Beyond adsorption energy and electronic properties, multiple-level descriptors have also been explored to capture more nuanced aspects of catalytic performance. Among others, Niu *et al.* proposed a descriptor, $\varphi = \frac{N_d}{\sqrt{E_{TM}}}$, where N_d is the number of TM-*d* orbital electrons, and E_{TM} is the electronegativity of TM atoms, to predict NRR activity[128]. Nong *et al.* proposed a descriptor, $\varphi = \theta\left[\chi_M + \alpha\sum_i (n_i \times \chi_i)\right] \Big/ \chi_N \, (i = C, N)$, which could predicate the *d*-band center of TMs anchored on C_3N, where θ is the number of TM atoms, χ_M, χ_C and χ_N are the electronegativity of TM, C and N atoms, respectively, n_i (i = C, N) represents the number of the nearest-neighbor C/N, and α is set as 1[128]. Zheng *et al.* developed another electronic descriptor, $\varphi = \frac{(\prod_{i=1}^{n} N_i)^{1/n}}{(\prod_{i=1}^{n} I_{1i})^{1/n}}$, where N is the *d* orbital electrons for metal atom or valence-electron for the neighboring N, I_1 is the first ionization energy of M or N, and *n* is the sum of the number of M or N. This descriptor considers the number of associated electrons and the first ionization energy of metal and nitrogen atoms, allowing effective estimation of NRR activity in TM trimers supported on N atoms-doped porous graphene (M_3-NG) systems[129].

These multiple-level descriptors, encompassing both electronic and atomic-level properties, offer promising avenues for application across various catalytic systems. However, a universally applicable descriptor for efficiently estimating NRR activity remains to be developed, indicating an ongoing need for further research.

SUMMARY AND PERSPECTIVE

Theoretical calculations play a crucial role not only in designing new catalysts but also in enhancing our understanding of reaction mechanisms. This insight provides meaningful guidance for creating efficient NRR catalysts capable of producing high-value-added chemicals. In this review, we have summarized recent theoretical advancements in SACs and SCCs for NRR.

Compared to traditional catalysts, SACs and SCCs feature well-defined active centers, making them more conducive to studying reaction mechanisms. Their structured active sites allow theoretical predictions to align closely with experimental findings, deepening our understanding of catalytic processes. SACs, with their unique structural characteristics, offer exceptional NRR catalytic performance, though their low production efficiency presents challenges for large-scale synthesis. SCCs, a recent extension of SACs, provide higher atomic loading and more flexible active sites, where multi-center synergy can optimize the interaction of the reactant and intermediate with the active sites, enhance mechanistic clarity, and ultimately improve catalytic performance. However, note that SCCs are not always superior to SACs for NRR, as exemplified recently by DACs, where the anticipated advantages over SACs are not consistently observed and are highly dependent on the specific properties of the metal[130].

In general, the coordination and electronic structure of the metal center, along with interactions between the support and the metal, are essential in determining the activity and stability of SACs and SCCs. Although SACs and SCCs have shown great promise in NRR applications, their performance is still insufficient to meet the demands of commercial-scale production.

With continuous in-depth study of the mechanism, we strongly believe that achievements in this field will continue to grow and inspire new advancements. Future breakthroughs in NRR catalyst development can focus on several areas, as outlined below.

First, advancing the synthesis of high-loading DACs and TACs is critical and faces significant challenges. Achieving precise atom or cluster dispersion without aggregation becomes increasingly difficult at higher loadings. Furthermore, identifying and optimizing suitable precursors and dispersion vectors requires meticulous effort and innovation. To address these issues, developing more efficient and robust synthesis strategies is imperative. Additionally, *in situ* characterization techniques are needed to precisely define active centers, enabling atomic-level investigations of structure-activity relationships and catalytic mechanisms. Such studies will provide invaluable insights into the interplay between catalyst structure and performance, guiding the rational design of high-loading SACs and SCCs.

Second, scaling the industrial application of SACs and SCCs presents formidable challenges, including high production costs driven by complex synthesis methods and the reliance on expensive precursors. Additionally, their stability and durability under rigorous industrial operating conditions require significant improvement. Future research will prioritize the development of cost-effective and scalable synthesis techniques alongside exploring novel support materials to bolster stability and longevity. Efforts will also optimize catalyst formulations tailored to specific industrial applications, ensuring both performance and practicality. As these technological advancements converge, SACs and SCCs are poised to transform industrial processes, unlocking new opportunities for efficient and sustainable energy conversion.

Third, it is essential to integrate theoretical calculations with experimental design to accelerate the research cycle. By combining theoretical and experimental efforts, researchers can promote the rational design of electrocatalysts with optimized activity, selectivity, and durability, generating significant economic and

social benefits. To bridge the gap between theoretical simulations and experimental outcomes, advanced computational chemistry methods and standardized approaches are also necessary.

Fourth, it is vital to develop generic activity descriptors that reveal the relationship between catalytic performance and material properties. A deeper understanding of these intrinsic relationships will support the advancement of SACs and SCCs, representing a new frontier in materials science. This progress not only offers a pathway to more efficient catalysts for NRR but also has broader implications for other multi-electron reactions.

In conclusion, single-atom and small-cluster catalysts mark a promising advance in the quest for efficient nitrogen reduction catalysts, and theoretical studies, especially high-throughput computations, ML, and descriptor-based screening techniques, are providing us with powerful tools to explore catalytic mechanisms and screen and design high-performance catalysts. While challenges remain - such as large-scale synthesis, commercialization and bridging theory with experiment - the synergy between theory and experiment is transforming catalyst design, and brings us closer to a future where SACs and SCCs drive sustainable NRR catalysis and open doors for other multi-electron reactions, blending curiosity with real-world impact.

DECLARATIONS

Authors' contributions

Conceived the idea and designed the project: Li, F., Chen, Z.
Performed data analysis and interpretation: Meng, H., Zhao, Y.
Supervised the project: Li, F.
Drafted the manuscript: Meng, H.
Revised and finalized the manuscript: Li, F., Chen, Z.

Availability of data and materials

Not applicable.

Financial support and sponsorship

This work was supported by the National Natural Science Foundation of China (12364038, 22103026), the young science and technology talents cultivation project of Inner Mongolia University (21200-5223708), the Industrial Technology Innovation Projects of Inner Mongolia Academy of Science and Technology of China (2023JSYD01002) and Science and Technology Plan Projects of Inner Mongolia Autonomous Region of China (2023KYPT0012).

Conflicts of interest

Chen, Z., an Associate Editor of *Journal of Materials Informatics*, and Li, F., the Guest Editor of the special issue, did not participate in any aspect of the editorial process, including reviewer selection, manuscript handling, or decision-making. The other authors declare that they have no conflicts of interest.

Ethical approval and consent to participate

Not applicable.

Consent for publication

Not applicable.

REFERENCES

1. Abbet, S.; Sanchez, A.; Heiz, U.; et al. Acetylene cyclotrimerization on supported size-selected Pd*n* clusters ($1 \leq n \leq 30$): one atom is enough! *J. Am. Chem. Soc.* **2000**, *122*, 3453-7. DOI
2. Li, Y.; Zhou, Z.; Yu, G.; Chen, W.; Chen, Z. CO catalytic oxidation on iron-embedded graphene: computational quest for low-cost nanocatalysts. *J. Phys. Chem. C.* **2010**, *114*, 6250-4. DOI
3. Lee, D. H.; Lee, W. J.; Lee, W. J.; Kim, S. O.; Kim, Y. H. Theory, synthesis, and oxygen reduction catalysis of Fe-porphyrin-like carbon nanotube. *Phys. Rev. Lett.* **2011**, *106*, 175502. DOI PubMed
4. Qiao, B.; Wang, A.; Yang, X.; et al. Single-atom catalysis of CO oxidation using Pt_1/FeO_x. *Nat. Chem.* **2011**, *3*, 634-41. DOI
5. Yang, X. F.; Wang, A.; Qiao, B.; Li, J.; Liu, J.; Zhang, T. Single-atom catalysts: a new frontier in heterogeneous. *Acc. Chem. Res.* **2013**, *46*, 1740-8. DOI PubMed
6. Akri, M.; Zhao, S.; Li, X.; et al. Atomically dispersed nickel as coke-resistant active sites for methane dry reforming. *Nat. Commun.* **2019**, *10*, 5181. DOI PubMed PMC
7. Han, B.; Guo, Y.; Huang, Y.; et al. Strong metal-support interactions between Pt single atoms and TiO_2. *Angew. Chem. Int. Ed. Engl.* **2020**, *59*, 11824-9. DOI
8. Jeong, H.; Lee, G.; Kim, B. S.; Bae, J.; Han, J. W.; Lee, H. Fully dispersed Rh ensemble catalyst to enhance low-temperature activity. *J. Am. Chem. Soc.* **2018**, *140*, 9558-65. DOI
9. Wang, Y.; Arandiyan, H.; Scott, J.; Aguey-Zinsou, K.; Amal, R. Single atom and nanoclustered Pt catalysts for selective CO_2 reduction. *ACS. Appl. Energy. Mater.* **2018**, *1*, 6781-9. DOI
10. Bai, S.; Liu, F.; Huang, B.; et al. High-efficiency direct methane conversion to oxygenates on a cerium dioxide nanowires supported rhodium single-atom catalyst. *Nat. Commun.* **2020**, *11*, 954. DOI PubMed PMC
11. Sun, C. N.; Wang, Z. L.; Lang, X. Y.; Wen, Z.; Jiang, Q. Synergistic effect of active sites of double-atom catalysts for nitrogen reduction reaction. *ChemSusChem* **2021**, *14*, 4593-600. DOI
12. Wang, P.; Chang, F.; Gao, W.; et al. Breaking scaling relations to achieve low-temperature ammonia synthesis through LiH-mediated nitrogen transfer and hydrogenation. *Nat. Chem.* **2017**, *9*, 64-70. DOI
13. Guo, X.; Gu, J.; Lin, S.; Zhang, S.; Chen, Z.; Huang, S. Tackling the activity and selectivity challenges of electrocatalysts toward the nitrogen reduction reaction via atomically dispersed biatom catalysts. *J. Am. Chem. Soc.* **2020**, *142*, 5709-21. DOI
14. Ouyang, Y.; Shi, L.; Bai, X.; Li, Q.; Wang, J. Breaking scaling relations for efficient CO_2 electrochemical reduction through dual-atom catalysts. *Chem. Sci.* **2020**, *11*, 1807-13. DOI PubMed PMC
15. Chen, Z.; Chen, L. X.; Yang, C. C.; Jiang, Q. Atomic (single, double, and triple atoms) catalysis: frontiers, opportunities, and challenges. *J. Mater. Chem. A.* **2019**, *7*, 3492-515. DOI
16. Galloway, J. N.; Townsend, A. R.; Erisman, J. W.; et al. Transformation of the nitrogen cycle: recent trends, questions, and potential solutions. *Science* **2008**, *320*, 889-92. DOI
17. Foster, S.; Bakovic, S. I. P.; Duda, R. D.; et al. Catalysts for nitrogen reduction to ammonia. *Nat. Catal.* **2018**, *1*, 490-500. DOI
18. Fu, X.; Zhang, J.; Kang, Y. Recent advances and challenges of electrochemical ammonia synthesis. *Chem. Catal.* **2022**, *2*, 2590-613. DOI
19. Iqbal, M. S.; Yao, Z.; Ruan, Y.; et al. Single-atom catalysts for electrochemical N_2 reduction to NH_3. *Rare. Met.* **2023**, *42*, 1075-97. DOI
20. Shang, H.; Liu, D. Atomic design of carbon-based dual-metal site catalysts for energy applications. *Nano. Res.* **2023**, *16*, 6477-506. DOI
21. He, T.; Puente-Santiago, A. R.; Xia, S.; Ahsan, M. A.; Xu, G.; Luque, R. Experimental and theoretical advances on single atom and atomic cluster-decorated low-dimensional platforms towards superior electrocatalysts. *Adv. Energy. Mater.* **2022**, *12*, 2200493. DOI
22. Chen, J.; Cao, H.; Chen, J.; et al. Heterogeneous two-atom single-cluster catalysts for the nitrogen electroreduction reaction. *J. Phys. Chem. C.* **2021**, *125*, 19821-30. DOI
23. Yan, Z.; Ji, M.; Xia, J.; Zhu, H. Recent advanced materials for electrochemical and photoelectrochemical synthesis of ammonia from dinitrogen: one step closer to a sustainable energy future. *Adv. Energy. Mater.* **2020**, *10*, 1902020. DOI
24. Qu, J.; Xiao, J.; Chen, H.; Liu, X.; Wang, T.; Zhang, Q. Orbital symmetry matching: achieving superior nitrogen reduction reaction over single-atom catalysts anchored on Mxene substrates. *Chinese. J. Catal.* **2021**, *42*, 288-96. DOI
25. Wang, T.; Abild-Pedersen, F. Achieving industrial ammonia synthesis rates at near-ambient conditions through modified scaling relations on a confined dual site. *Proc. Natl. Acad. Sci. U. S. A.* **2021**, *118*, e2106527118. DOI
26. Yao, Y.; Zhu, S.; Wang, H.; Li, H.; Shao, M. A spectroscopic study of electrochemical nitrogen and nitrate reduction on rhodium surfaces. *Angew. Chem. Int. Ed. Engl.* **2020**, *59*, 10479-83. DOI
27. Ling, C.; Zhang, Y.; Li, Q.; Bai, X.; Shi, L.; Wang, J. New mechanism for N_2 reduction: the essential role of surface hydrogenation. *J. Am. Chem. Soc.* **2019**, *141*, 18264-70. DOI
28. Abghoui, Y.; Skúlason, E. Onset potentials for different reaction mechanisms of nitrogen activation to ammonia on transition metal nitride electro-catalysts. *Catal. Today.* **2017**, *286*, 69-77. DOI

29. Abghoui, Y.; Skúlason, E. Computational predictions of catalytic activity of zincblende (110) surfaces of metal nitrides for electrochemical ammonia synthesis. *J. Phys. Chem. C.* **2017**, *121*, 6141-51. DOI
30. Martín, A. J.; Shinagawa, T.; Pérez-Ramírez, J. Electrocatalytic reduction of nitrogen: from haber-bosch to ammonia artificial leaf. *Chem* **2019**, *5*, 263-83. DOI
31. Shaw, S.; Lukoyanov, D.; Danyal, K.; Dean, D. R.; Hoffman, B. M.; Seefeldt, L. C. Nitrite and hydroxylamine as nitrogenase substrates: mechanistic implications for the pathway of N_2 reduction. *J. Am. Chem. Soc.* **2014**, *136*, 12776-83. DOI PubMed PMC
32. Zhao, J.; Chen, Z. Single Mo atom supported on defective boron nitride monolayer as an efficient electrocatalyst for nitrogen fixation: a computational study. *J. Am. Chem. Soc.* **2017**, *139*, 12480-7. DOI
33. Wang, Z.; Yu, Z.; Zhao, J. Computational screening of a single transition metal atom supported on the C_2N monolayer for electrochemical ammonia synthesis. *Phys. Chem. Chem. Phys.* **2018**, *20*, 12835-44. DOI
34. Zhao, J.; Zhao, J.; Cai, Q. Single transition metal atom embedded into a MoS_2 nanosheet as a promising catalyst for electrochemical ammonia synthesis. *Phys. Chem. Chem. Phys.* **2018**, *20*, 9248-55. DOI
35. Zhai, X.; Yan, H.; Ge, G.; et al. The single-Mo-atom-embedded-graphdiyne monolayer with ultra-low onset potential as high efficient electrocatalyst for N_2 reduction reaction. *Appl. Surf. Sci.* **2020**, *506*, 144941. DOI
36. Liu, S.; Liu, Y.; Gao, X.; et al. Two-dimensional transition metal porphyrin sheets as a promising single-atom-catalyst for dinitrogen electrochemical reduction to ammonia: a theoretical study. *J. Phys. Chem. C.* **2020**, *124*, 1492-9. DOI
37. Xu, L.; Yang, L. M.; Ganz, E. Electrocatalytic reduction of N_2 using metal-doped borophene. *ACS. Appl. Mater. Interfaces.* **2021**, *13*, 14091-101. DOI
38. Li, C.; Liu, X.; Wu, D.; Xu, H.; Fan, G. Theoretical study of transition metal doped α-borophene nanosheet as promising electrocatalyst for electrochemical reduction of N_2. *Comput. Theor. Chem.* **2022**, *1213*, 113732. DOI
39. Ling, C.; Bai, X.; Ouyang, Y.; Du, A.; Wang, J. Single molybdenum atom anchored on N-doped carbon as a promising electrocatalyst for nitrogen reduction into ammonia at ambient conditions. *J. Phys. Chem. C.* **2018**, *122*, 16842-7. DOI
40. Zhao, W.; Zhang, L.; Luo, Q.; et al. Single $Mo_1(Cr_1)$ atom on nitrogen-doped graphene enables highly selective electroreduction of nitrogen into ammonia. *ACS. Catal.* **2019**, *9*, 3419-25. DOI
41. Liu, P.; Fu, C.; Li, Y.; Wei, H. Theoretical screening of single atoms anchored on defective graphene for electrocatalytic N_2 reduction reactions: a DFT study. *Phys. Chem. Chem. Phys.* **2020**, *22*, 9322-9. DOI
42. Niu, H.; Wang, X.; Shao, C.; Zhang, Z.; Guo, Y. Computational screening single-atom catalysts supported on g-CN for N_2 reduction: high activity and selectivity. *ACS. Sustainable. Chem. Eng.* **2020**, *8*, 13749-58. DOI
43. Li, L.; Li, B.; Guo, Q.; Li, B. Theoretical screening of single-atom-embedded MoSSe nanosheets for electrocatalytic N_2 fixation. *J. Phys. Chem. C.* **2019**, *123*, 14501-7. DOI
44. Cui, Q.; Qin, G.; Wang, W.; K, R. G.; Du, A.; Sun, Q. Mo-based 2D MOF as a highly efficient electrocatalyst for reduction of N_2 to NH_3: a density functional theory study. *J. Mater. Chem. A.* **2019**, *7*, 14510-8. DOI
45. Huang, Y.; Yang, T.; Yang, L.; et al. Graphene–boron nitride hybrid-supported single Mo atom electrocatalysts for efficient nitrogen reduction reaction. *J. Mater. Chem. A.* **2019**, *7*, 15173-80. DOI
46. Zhou, H. Y.; Li, J. C.; Wen, Z.; Jiang, Q. Tuning the catalytic activity of a single Mo atom supported on graphene for nitrogen reduction *via* Se atom doping. *Phys. Chem. Chem. Phys.* **2019**, *21*, 14583-8. DOI
47. Ou, P.; Zhou, X.; Meng, F.; Chen, C.; Chen, Y.; Song, J. Single molybdenum center supported on N-doped black phosphorus as an efficient electrocatalyst for nitrogen fixation. *Nanoscale* **2019**, *11*, 13600-11. DOI
48. Qi, J.; Gao, L.; Wei, F.; Wan, Q.; Lin, S. Design of a high-performance electrocatalyst for N_2 conversion to NH_3 by trapping single metal atoms on stepped CeO_2. *ACS. Appl. Mater. Interfaces.* **2019**, *11*, 47525-34. DOI
49. Gao, L.; Wang, F.; Yu, M.; et al. A novel phosphotungstic acid-supported single metal atom catalyst with high activity and selectivity for the synthesis of NH_3 from electrochemical N_2 reduction: a DFT prediction. *J. Mater. Chem. A.* **2019**, *7*, 19838-45. DOI
50. Talib, S. H.; Yu, X.; Lu, Z.; et al. A polyoxometalate cluster-based single-atom catalyst for NH_3 synthesis *via* an enzymatic mechanism. *J. Mater. Chem. A.* **2022**, *10*, 6165-77. DOI
51. Li, Q.; Liu, C.; Qiu, S.; et al. Exploration of iron borides as electrochemical catalysts for the nitrogen reduction reaction. *J. Mater. Chem. A.* **2019**, *7*, 21507-13. DOI
52. Ma, Z.; Cui, Z.; Xiao, C.; et al. Theoretical screening of efficient single-atom catalysts for nitrogen fixation based on a defective BN monolayer. *Nanoscale* **2020**, *12*, 1541-50. DOI
53. Hu, J.; Tian, L.; Wang, H.; et al. Theoretical screening of single-atom electrocatalysts of MXene-supported 3d-metals for efficient nitrogen reduction. *Chinese. J. of. Catal.* **2023**, *52*, 252-62. DOI
54. Zhang, N.; Gao, Y.; Ma, L.; et al. Single transition metal atom anchored on g-C_3N_4 as an electrocatalyst for nitrogen fixation: a computational study. *Int. J. Hydrogen. Energy.* **2023**, *48*, 7621-31. DOI
55. Sahoo, S. K.; Heske, J.; Antonietti, M.; Qin, Q.; Oschatz, M.; Kühne, T. D. Electrochemical N_2 reduction to ammonia using single Au/Fe atoms supported on nitrogen-doped porous carbon. *ACS. Appl. Energy. Mater.* **2020**, *3*, 10061-9. DOI PubMed PMC
56. Choi, C.; Back, S.; Kim, N.; Lim, J.; Kim, Y.; Jung, Y. Suppression of hydrogen evolution reaction in electrochemical N_2 reduction using single-atom catalysts: a computational guideline. *ACS. Catal.* **2018**, *8*, 7517-25. DOI
57. Zhu, H.; Hu, Y.; Wei, S.; Hua, D. Single-metal atom anchored on boron monolayer (β_{12}) as an electrocatalyst for nitrogen reduction into ammonia at ambient conditions: a first-principles study. *J. Phys. Chem. C.* **2019**, *123*, 4274-81. DOI
58. Feng, Z.; Tang, Y.; Chen, W.; et al. Graphdiyne coordinated transition metals as single-atom catalysts for nitrogen fixation. *Phys.*

Chem. Chem. Phys. **2020**, *22*, 9216-24. DOI

59. Xu, Z.; Song, R.; Wang, M.; Zhang, X.; Liu, G.; Qiao, G. Single atom-doped arsenene as electrocatalyst for reducing nitrogen to ammonia: a DFT study. *Phys. Chem. Chem. Phys.* **2020**, *22*, 26223-30. DOI
60. Zhang, J.; Yang, H.; Liu, B. Coordination engineering of single-atom catalysts for the oxygen reduction reaction: a review. *Adv. Energy. Mater.* **2021**, *11*, 2002473. DOI
61. Ikeda, T.; Aratani, N.; Osuka, A. Synthesis of extremely pi-extended porphyrin tapes from hybrid meso-meso linked porphyrin arrays: an approach towards the conjugation length. *Chem. Asian. J.* **2009**, *4*, 1248-56. DOI PubMed
62. Nakamura, Y.; Aratani, N.; Shinokubo, H.; et al. A directly fused tetrameric porphyrin sheet and its anomalous electronic properties that arise from the planar cyclooctatetraene core. *J. Am. Chem. Soc.* **2006**, *128*, 4119-27. DOI
63. Yang, L.; Chen, F.; Wu, M.; Song, E.; Xiao, B.; Jiang, Q. Mo decoration on graphene edge for nitrogen fixation: a computational investigation. *Appl. Surf. Sci.* **2021**, *568*, 150867. DOI
64. Patel, A. M.; Ringe, S.; Siahrostami, S.; Bajdich, M.; Nørskov, J. K.; Kulkarni, A. R. Theoretical approaches to describing the oxygen reduction reaction activity of single-atom catalysts. *J. Phys. Chem. C.* **2018**, *122*, 29307-18. DOI
65. Rodriguez, M. M.; Bill, E.; Brennessel, W. W.; Holland, P. L. N_2 reduction and hydrogenation to ammonia by a molecular iron-potassium complex. *Science* **2011**, *334*, 780-3. DOI
66. Wang, T.; Guo, Z.; Zhang, X.; et al. Recent progress of iron-based electrocatalysts for nitrogen reduction reaction. *J. Mater. Sci. Technol.* **2023**, *140*, 121-34. DOI
67. Li, X. F.; Li, Q. K.; Cheng, J.; et al. Conversion of dinitrogen to ammonia by FeN_3-embedded graphene. *J. Am. Chem. Soc.* **2016**, *138*, 8706-9. DOI
68. Li, B.; Du, W.; Wu, Q.; Dai, Y.; Huang, B.; Ma, Y. Coronene-based 2D metal–organic frameworks: a new family of promising single-atom catalysts for nitrogen reduction reaction. *J. Phys. Chem. C.* **2021**, *125*, 20870-6. DOI
69. Sippel, D.; Rohde, M.; Netzer, J.; et al. A bound reaction intermediate sheds light on the mechanism of nitrogenase. *Science* **2018**, *359*, 1484-9. DOI
70. Liu, C.; Li, Q.; Zhang, J.; Jin, Y.; Macfarlane, D. R.; Sun, C. Conversion of dinitrogen to ammonia on Ru atoms supported on boron sheets: a DFT study. *J. Mater. Chem. A.* **2019**, *7*, 4771-6. DOI
71. Yin, H.; Li, S.; Gan, L.; Wang, P. Pt-embedded in monolayer g-C_3N_4 as a promising single-atom electrocatalyst for ammonia synthesis. *J. Mater. Chem. A.* **2019**, *7*, 11908-14. DOI
72. Chen, Z.; Zhao, J.; Cabrera, C. R.; Chen, Z. Computational screening of efficient single-atom catalysts based on graphitic carbon nitride (g-C_3N_4) for nitrogen electroreduction. *Small. Methods.* **2019**, *3*, 1800368. DOI
73. Wang, M.; Huang, Y.; Ma, F.; et al. Theoretical insights into the mechanism of nitrogen-to-ammonia electroreduction on TM/g-C_9N_{10} . *Mol. Cataly.* **2023**, *547*, 113391. DOI
74. Saeidi, N.; Esrafili, M. D.; Sardroodi, J. J. Electrochemical reduction of N_2 to NH_3 using a co-atom stabilized on defective N-doped graphene: a computational study. *ChemistrySelect* **2019**, *4*, 12216-26. DOI
75. Wu, J.; Li, J. H.; Yu, Y. X. Single Nb or W atom-embedded BP monolayers as highly selective and stable electrocatalysts for nitrogen fixation with low-onset potentials. *ACS. Appl. Mater. Interfaces.* **2021**, *13*, 10026-36. DOI PubMed
76. Gao, Y.; Yang, Y.; Hao, L.; et al. Single Nb atom modified anatase TiO_2(110) for efficient electrocatalytic nitrogen reduction reaction. *Chem. Catal.* **2022**, *2*, 2275-88. DOI
77. Li, Q.; Qiu, S.; Liu, C.; et al. Computational design of single-molybdenum catalysts for the nitrogen reduction reaction. *J. Phys. Chem. C.* **2019**, *123*, 2347-52. DOI
78. Jiao, D.; Liu, Y.; Cai, Q.; Zhao, J. Coordination tunes the activity and selectivity of the nitrogen reduction reaction on single-atom iron catalysts: a computational study. *J. Mater. Chem. A.* **2021**, *9*, 1240-51. DOI
79. Wang, X.; Yang, L. Efficient modulation of the catalytic performance of electrocatalytic nitrogen reduction with transition metals anchored on N/O-codoped graphene by coordination engineering. *J. Mater. Chem. A.* **2022**, *10*, 1481-96. DOI
80. Tang, Y.; Wang, Y.; Cheng, X.; Zhang, H. Single vanadium atom achored on sulfur-doped graphene as an efficient electrocatalyst toward the nitrogen reduction reaction: a computational view. *J. Phys. Chem. C.* **2023**, *127*, 24574-82. DOI
81. Di Liberto G, Giordano L, Pacchioni G. Predicting the stability of single-atom catalysts in electrochemical reactions. *ACS. Catal.* **2024**, *14*, 45-55. DOI
82. Chu, Z.; Kang, X.; Duan, X. Single metal atom anchored on a CN monolayer as an excellent electrocatalyst for the nitrogen reduction reaction. *Phys. Chem. Chem. Phys.* **2021**, *23*, 2658-62. DOI
83. Song, R.; Yang, J.; Wang, M.; et al. Theoretical study on P-coordinated metal atoms embedded in arsenene for the conversion of nitrogen to ammonia. *ACS. Omega.* **2021**, *6*, 8662-71. DOI PubMed PMC
84. Wang, X.; Zhang, Q.; Hao, W.; Fang, C.; Zhou, J.; Xu, J. A novel porous graphitic carbon nitride (g-C_7N_3) substrate: prediction of metal-based π–d conjugated nanosheets toward the highly active and selective electrocatalytic nitrogen reduction reaction. *J. Mater. Chem. A.* **2022**, *10*, 15036-50. DOI
85. Song, W.; Xie, K.; Wang, J.; Guo, Y.; He, C.; Fu, L. Density functional theory study of transition metal single-atoms anchored on graphyne as efficient electrocatalysts for the nitrogen reduction reaction. *Phys. Chem. Chem. Phys.* **2021**, *23*, 10418-28. DOI
86. Zhao, Y.; Qu, J.; Li, H.; et al. Atomically dispersed uranium enables an unprecedentedly high NH_3 yield rate. *Nano. Lett.* **2022**, *22*, 4475-81. DOI
87. Meng, Q.; Liu, L.; Song, D.; Wang, S.; Qin, R.; Fu, G. Flexible iron clusters promoting ammonia synthesis: a density functional

theory prediction. *J. Phys. Chem. Lett.* **2024**, *15*, 10623-8. DOI

88. Li, R.; Wang, D. Superiority of dual-atom catalysts in electrocatalysis: one step further than single-atom catalysts. *Adv. Energy. Mater.* **2022**, *12*, 2103564. DOI
89. Qian, Y.; Liu, Y.; Zhao, Y.; Zhang, X.; Yu, G. Single vs double atom catalyst for N_2 activation in nitrogen reduction reaction: a DFT perspective. *EcoMat* **2020**, *2*, e12014. DOI
90. Chen, Z. W.; Yan, J.; Jiang, Q. Single or double: which is the altar of atomic catalysts for nitrogen reduction reaction? *Small. Methods.* **2019**, *3*, 1800291. DOI
91. Zhang, X.; Chen, A.; Zhang, Z.; Zhou, Z. Double-atom catalysts: transition metal dimer-anchored C_2N monolayers as N_2 fixation electrocatalysts. *J. Mater. Chem. A.* **2018**, *6*, 18599-604. DOI
92. Guo, R.; Hu, M.; Zhang, W.; He, J. Boosting electrochemical nitrogen reduction performance over binuclear Mo atoms on N-doped nanoporous graphene: a theoretical investigation. *Molecules* **2019**, *24*, 1777. DOI PubMed PMC
93. Zhang, Z.; Xu, X. g-C_3N_4-supported metal-pair catalysts toward efficient electrocatalytic nitrogen reduction: a computational evaluation. *Adv. Theory. Simul.* **2022**, *5*, 2100579. DOI
94. Yang, Y.; Hu, C.; Shan, J.; et al. Electrocatalytically activating and reducing N_2 molecule by tuning activity of local hydrogen radical. *Angew. Chem. Int. Ed. Engl.* **2023**, *62*, e202300989. DOI
95. Wu, Y.; He, C.; Zhang, W. Building up a general selection strategy and catalytic performance prediction expressions of heteronuclear double-atom catalysts for N_2 reduction. *J. Energy. Chem.* **2023**, *82*, 375-86. DOI
96. Zheng, X.; Yao, Y.; Wang, Y.; Liu, Y. Tuning the electronic structure of transition metals embedded in nitrogen-doped graphene for electrocatalytic nitrogen reduction: a first-principles study. *Nanoscale* **2020**, *12*, 9696-707. DOI
97. He, T.; Puente, S. A. R.; Du, A. Atomically embedded asymmetrical dual-metal dimers on N-doped graphene for ultra-efficient nitrogen reduction reaction. *J. Catal.* **2020**, *388*, 77-83. DOI
98. Li, Y.; Zhang, Q.; Li, C.; et al. Atomically dispersed metal dimer species with selective catalytic activity for nitrogen electrochemical reduction. *J. Mater. Chem. A.* **2019**, *7*, 22242-7. DOI
99. Zheng, G.; Li, L.; Hao, S.; Zhang, X.; Tian, Z.; Chen, L. Double atom catalysts: heteronuclear transition metal dimer anchored on nitrogen-doped graphene as superior electrocatalyst for nitrogen reduction reaction. *Adv. Theory. Simul.* **2020**, *3*, 2000190. DOI
100. Ma, D.; Zeng, Z.; Liu, L.; Jia, Y. Theoretical screening of the transition metal heteronuclear dimer anchored graphdiyne for electrocatalytic nitrogen reduction. *J. Energy. Chem.* **2021**, *54*, 501-9. DOI
101. Cui, C.; Zhang, H.; Cheng, R.; Huang, B.; Luo, Z. On the nature of three-atom metal cluster catalysis for N_2 reduction to ammonia. *ACS. Catal.* **2022**, *12*, 14964-75. DOI
102. Liu, J. C.; Ma, X. L.; Li, Y.; Wang, Y. G.; Xiao, H.; Li, J. Heterogeneous Fe_3 single-cluster catalyst for ammonia synthesis via an associative mechanism. *Nat. Commun.* **2018**, *9*, 1610. DOI PubMed PMC
103. Chen, Z. W.; Chen, L. X.; Jiang, M.; et al. A triple atom catalyst with ultrahigh loading potential for nitrogen electrochemical reduction. *J. Mater. Chem. A.* **2020**, *8*, 15086-93. DOI
104. Guo, R.; An, W.; Liu, M.; et al. Modulating the coordination environment of active site structure for enhanced electrochemical nitrogen reduction: the mechanistic insight and an effective descriptor. *Appl. Surf. Sci.* **2024**, *644*, 158799. DOI
105. Han, B.; Meng, H.; Li, F.; Zhao, J. Fe_3 cluster anchored on the C_2N monolayer for efficient electrochemical nitrogen fixation. *Catalysts* **2020**, *10*, 974. DOI
106. Han, B.; Li, F. Regulating the electrocatalytic performance for nitrogen reduction reaction by tuning the N contents in $Fe_3@N_xC_{20-x}$ (x = 0~4): a DFT exploration. *J. Mater. Inf.* **2023**, *3*, 24. DOI
107. Chen, S.; Gao, Y.; Wang, W.; Prezhdo, O. V.; Xu, L. Prediction of three-metal cluster catalysts on two-dimensional W_2N_3 support with integrated descriptors for electrocatalytic nitrogen reduction. *ACS. Nano.2023*, 1522-32. DOI
108. Pei, W.; Zhang, W.; Yu, X.; et al. Computational design of spatially confined triatomic catalysts for nitrogen reduction reaction. *J. Mater. Inf.* **2023**, *3*, 26. DOI
109. Pei, W.; Hou, L.; Yu, X.; et al. Graphitic carbon nitride supported trimeric metal clusters as electrocatalysts for N_2 reduction reaction. *J. Catal.* **2024**, *429*, 115232. DOI
110. Zhang, H.; Cui, C.; Luo, Z. MoS_2-supported Fe_2 clusters catalyzing nitrogen reduction reaction to produce ammonia. *J. Phys. Chem. C.* **2020**, *124*, 6260-6. DOI
111. Anis, I.; Amin, S.; Rather, G. M.; Dar, M. A. N_2 activation and reduction on graphdiyne supported single, double, and triple boron atom catalysts: a first principles investigation. *ChemistrySelect* **2023**, *8*, e202300993. DOI
112. Wang, X.; Lin, L.; Li, B. First principles study of double boron atoms supported on graphitic carbon nitride (g-C_3N_4) for nitrogen electroreduction. *Crystals* **2022**, *12*, 1744. DOI
113. Rasool, A.; Anis, I.; Bhat, S. A.; Dar, M. A. Optimizing the NRR activity of single and double boron atom catalysts using a suitable support: a first principles investigation. *Phys. Chem. Chem. Phys.* **2023**, *25*, 22275-85. DOI PubMed
114. Hu, Y.; Chen, J.; Wei, Z.; He, Q.; Zhao, Y. Recent advances and applications of machine learning in electrocatalysis. *J. Mater. Inf.* **2023**, *3*, 18. DOI
115. Lu, Y.; Fang, C.; Zhang, Q.; et al. Single-atom catalytic N_2 fixation with integrated descriptors on a novel π-π conjugated graphitic carbon nitride (g-$C_{13}N_{15}$) platform obtained by self-doping design: prediction of ultrahigh activity and desirable selectivity. *J. Power. Sources.* **2024**, *595*, 234030. DOI
116. Lv, X.; Wei, W.; Huang, B.; Dai, Y.; Frauenheim, T. High-throughput screening of synergistic transition metal dual-atom catalysts

for efficient nitrogen fixation. *Nano. Lett.* **2021**, *21*, 1871-8. DOI

117. Sun, J.; Xia, P.; Lin, Y.; et al. Theoretical exploration of the nitrogen fixation mechanism of two-dimensional dual-metal TM_1TM_2@C_9N_4 electrocatalysts. *Nanoscale. Horiz.* **2023**, *8*, 211-23. DOI
118. Sun, J.; Chen, A.; Guan, J.; et al. Interpretable machine learning-assisted high-throughput screening for understanding NRR electrocatalyst performance modulation between active center and C-N coordination. *Energy. Environ. Mater.* **2024**, *7*, e12693. DOI
119. Zhang, S.; Lu, S.; Zhang, P.; et al. Accelerated discovery of single-atom catalysts for nitrogen fixation via machine learning. *Energy. Environ. Mater.* **2023**, *6*, e12304. DOI
120. Zhang, Y.; Wang, Y.; Ma, N.; Fan, J. Directly predicting N_2 electroreduction reaction free energy using interpretable machine learning with non-DFT calculated features. *J. Energy. Chem.* **2024**, *97*, 139-48. DOI
121. Chen, C.; Cao, J.; Yin, W.; Zhang, Q.; Yao, Y.; Wei, X. Single transition metal atom modified $MoSe_2$ as a promising electrocatalyst for nitrogen fixation: a first-principles study. *Chem. Phys. Lett.* **2021**, *780*, 138939. DOI
122. Ma, D.; Zeng, Z.; Liu, L.; Huang, X.; Jia, Y. Computational evaluation of electrocatalytic nitrogen reduction on TM single-, double-, and triple-atom catalysts (TM = Mn, Fe, Co, Ni) based on graphdiyne monolayers. *J. Phys. Chem. C.* **2019**, *123*, 19066-76. DOI
123. Ren, C.; Jiang, Q.; Lin, W.; Zhang, Y.; Huang, S.; Ding, K. Density functional theory study of single-atom V, Nb, and Ta catalysts on graphene and carbon nitride for selective nitrogen reduction. *ACS. Appl. Nano. Mater.* **2020**, *3*, 5149-59. DOI
124. Luo, Y.; Li, M.; Dai, Y.; et al. Transition metal-modified Co_4 clusters supported on graphdiyne as an effective nitrogen reduction reaction electrocatalyst. *Inorg. Chem.* **2021**, *60*, 18251-9. DOI
125. Liu, S.; Liu, J. Rational design of highly efficient electrocatalytic single-atom catalysts for nitrogen reduction on nitrogen-doped graphene and g-C_2N supports. *J. Power. Sources.* **2022**, *535*, 231449. DOI
126. Wang, J.; Luo, Z.; Zhang, X.; et al. Single transition metal atom anchored on VSe_2 as electrocatalyst for nitrogen reduction reaction. *Appl. Surf. Sci.* **2022**, *580*, 152272. DOI
127. Zhang, Y.; Wang, X.; Liu, T.; et al. Charge and spin communication between dual metal single-atom sites on C_2N sheets: regulating electronic spin moments of Fe atoms for N_2 activation and reduction. *J. Mater. Chem. A.* **2022**, *10*, 23704-11. DOI
128. Nong, W.; Qin, S.; Huang, F.; et al. Designing C_3N-supported single atom catalysts for efficient nitrogen reduction based on descriptor of catalytic activity. *Carbon* **2021**, *182*, 297-306. DOI
129. Zheng, X.; Liu, Y.; Yao, Y. Trimetallic single-cluster catalysts for electrochemical nitrogen reduction reaction: activity prediction, mechanism, and electronic descriptor. *Chem. Eng. J.* **2021**, *426*, 130745. DOI
130. Barlocco, I.; Spotti, M.; Liberto, G. D.; Pacchioni, G. Electrochemical nitrogen reduction reaction from ab initio thermodynamics: single versus dual atom catalysts. *Adv. Theory. Simul.* **2024**, *7*, 2400536. DOI